

Momentum dependence of near-threshold photoproduction of Ξ^- hyperons off nuclei and their properties in the nuclear medium

E. Ya. Paryev^{1,2}

¹*Institute for Nuclear Research, Russian Academy of Sciences,
Moscow 117312, Russia*

²*Institute for Theoretical and Experimental Physics,
Moscow 117218, Russia*

Abstract

We study the near-threshold inclusive photoproduction of Ξ^- hyperons off ^{12}C and ^{184}W target nuclei within a first-collision model relying on the nuclear spectral function and including incoherent Ξ^- production in direct elementary $\gamma p \rightarrow K^+ K^+ \Xi^-$ and $\gamma n \rightarrow K^+ K^0 \Xi^-$ processes. The model takes into account the impact of the nuclear effective scalar K^+ , K^0 , Ξ^- and their Coulomb potentials on these processes as well as the absorption of final Ξ^- hyperons in nuclear matter, the binding of intranuclear nucleons and their Fermi motion. We calculate the absolute differential cross sections and their ratios for the production of Ξ^- hyperons off these nuclei at laboratory polar angles $\leq 45^\circ$ by photons with energies of 2.5 and 3.0 GeV, with and without imposing the phase space constraints on the Ξ^- emission angle in the respective γp center-of-mass system. We also calculate the momentum dependence of the transparency ratio for Ξ^- hyperons for the $^{184}\text{W}/^{12}\text{C}$ combination at these photon energies. We show that the Ξ^- momentum distributions (absolute and relative) at the adopted initial photon energies possess a definite sensitivity to the considered changes in the scalar Ξ^- nuclear mean-field potential at saturation density ρ_0 in the low-momentum range of 0.1–0.8 GeV/c. This would permit evaluating the Ξ^- potential in this momentum range experimentally. We also demonstrate that the momentum dependence of the transparency ratio for Ξ^- hyperons for both photon energies can hardly be used to determine this potential reliably. Therefore, the precise measurements of the differential cross sections (absolute and relative) for inclusive Ξ^- hyperon photoproduction on nuclei near threshold in a dedicated experiment at the CEBAF facility will provide valuable information on the Ξ^- in-medium properties, which will be supplementary to that inferred from studying of the (K^-, K^+) reactions at initial momenta of 1.6–1.8 GeV/c.

1 Introduction

The investigation of the Ξ^-N and Ξ^- -nucleus interactions has received considerable interest in recent years (see, for example, [1]). The knowledge of these interactions is important for understanding the neutron star properties and the properties of such exotic nuclear systems as the Ξ^- hypernuclei [1] as well as for constraining the equation of state (EoS) of dense nuclear matter [2]. Mostly, the study of Ξ^- hypernuclei provide a valuable information on them at low energies. Presently, the possibility to extract information on the Ξ^-N interaction also from studying the momentum correlations of p and Ξ^- , produced in high-energy heavy ion collisions, as well as from lattice QCD calculations becomes feasible (see, for instance, [3]). An information inferred in Refs. [4] and [5–9] from old and new emulsion hypernuclear data, from missing-mass measurements [10–14] in the inclusive (K^-,K^+) reactions on nuclear targets at incident momenta of 1.6–1.8 GeV/c, from the analysis the results of these measurements in the Ξ^- bound and quasi-free regions in Refs. [15–17] using the DWIA method as well as the theoretical predictions [18–31] indicate that the Ξ^- hyperon feels only a moderately attractive low-energy potential in nuclei, the depth of which is about of $-(10-20)$ MeV at saturation nuclear density ρ_0 . To improve significantly our knowledge on the low-energy Ξ^-N interaction the high-precision data on the Ξ^- hypernuclei are needed. It is expected that such data on the missing-mass spectra for the $^{12}\text{C}(K^-,K^+)$ reaction close to the Ξ^- production threshold and the X-ray data on the level shifts and width broadening of the Ξ^- atomic states in the Ξ^- atoms will become available soon from the E70 and E03 experiments at the J-PARC [32]. It is worthwhile to point out that the situation with the Ξ^- nuclear potential at finite momenta is still unclear at present, in spite of a lot theoretical activity [22–27] in this field. In addition to the above-mentioned (K^-,K^+) reactions on nuclear targets at beam momenta of 1.6–1.8 GeV/c, the medium modification of the Ξ^- hyperon could be probed directly, as was shown in Ref. [33], via the another inclusive near-threshold (K^-,Ξ^-) reactions on nuclei. This modification can also be sought by studying the cascade hyperon production off nuclei in photon-induced reactions at energies close to the threshold energy (≈ 2.4 GeV) for its production off a free target nucleon at rest. Owing to a negligible strength of initial-state photon interaction in relation to hadron-nucleus interaction, photon-nucleus reactions appear to be a more useful tool for studying in-medium properties of Ξ^- hyperons and their interactions in cold nuclear matter both at the threshold and at finite momenta. In this context, the main aim of the present study is to continue the investigation of the in-medium properties of the Ξ^- hyperons via their photoproduction off nuclei. We give the predictions for the absolute differential cross sections and their ratios for near-threshold photoproduction of Ξ^- hyperons off ^{12}C and ^{184}W nuclei at laboratory angles of $\leq 45^\circ$ by incident photons with energies of 2.5 and 3.0 GeV within three different scenarios for the effective scalar mean-field nuclear potential that Ξ^- hyperon feels in the medium. These predictions have been obtained in the framework of the first-collision model based on a nuclear spectral function and developed in Ref. [33] for the description of the inclusive Ξ^- hyperon production on nuclei in near-threshold antikaon-induced reactions and modified to the case of photon-nucleus reactions. Their comparison with the respective data, which could be collected in the future dedicated experiment, will provide a deeper insight into the Ξ^- in-medium properties. Information obtained from this comparison will supplement that inferred from the (K^-,K^+) reactions on nuclear targets. Such experiment might be performed at the CEBAF facility, especially in view of the fact that the exclusive photoproduction of Ξ^- and Ξ^0 hyperons in elementary reactions $\gamma p \rightarrow K^+K^+\Xi^-$ and $\gamma p \rightarrow K^+K^+\pi^-\Xi^0$ has already been investigated here for near-threshold photon energies using the CLAS [34–36] and GlueX [37] detectors.

2 Formalism: direct Ξ^- hyperon production mechanism in nuclei

Since we are interested in the incident photon energy region only up to 3.0 GeV, we assume that direct production of Ξ^- hyperons in photon-induced reactions in this region can proceed in the following γp and γn elementary processes, having the lowest threshold for their free production (≈ 2.4 GeV):

$$\gamma + p \rightarrow K^+ + K^+ + \Xi^-, \quad (1)$$

$$\gamma + n \rightarrow K^+ + K^0 + \Xi^-. \quad (2)$$

We can disregard the contribution to the ground state $\Xi^- = \Xi(1320)^-$ production from the elementary channels $\gamma N \rightarrow KK\Xi^-\pi$ and $\gamma N \rightarrow KK\Xi(1530)^- \rightarrow KK\Xi^-\pi^0$, in which the Ξ^- hyperons are produced directly and through the decay of the intermediate first excited state $\Xi(1530)^-$, at considered incident energies owing to their larger thresholds (≈ 2.7 and 2.9 GeV, respectively) in free γN collisions.

According [33, 38], we simplify the subsequent calculations via accounting for the in-medium modifications of the final K^+ , K^0 mesons and Ξ^- hyperons, involved in the production processes (1), (2), in terms of their average in-medium masses $\langle m_{K^+}^* \rangle$, $\langle m_{K^0}^* \rangle$ and $\langle m_{\Xi^-}^* \rangle$ in the in-medium cross sections of these processes, which are defined as:

$$\langle m_h^* \rangle = m_h + U_h \frac{\langle \rho_N \rangle}{\rho_0} + V_{ch}(\bar{r}), \quad (3)$$

where h denotes K^+ , K^0 and Ξ^- . Here, m_h is the bare hadron mass, U_h is its effective scalar nuclear potential which it feels at normal nuclear matter density ρ_0 , $\langle \rho_N \rangle$ is the average nucleon density and $V_{ch}(\bar{r})$ is the charged hadron Coulomb potential ¹⁾ corresponding to the interaction between the point hadron h and the uniformly charged spherical core of charge Z and taken at a point \bar{r} at which the local nucleon density is equal to the average density ²⁾. For the K^+ scalar potential U_{K^+} we will use the following option: $U_{K^+} = +22$ MeV [39, 40]. The same option will be adopted for the K^0 nuclear potential U_{K^0} in the case of ^{12}C target nucleus, i.e.: $U_{K^0} = U_{K^+} = +22$ MeV [33, 40–42]. And in the case of ^{184}W nucleus for the K^0 scalar potential U_{K^0} we will use the following value: $U_{K^0} = +40$ MeV [33, 40, 41].

Now, we specify the effective scalar mean-field Ξ^- hyperon potential U_{Ξ^-} in Eq. (3). We assume that this potential is the same for both considered target nuclei ^{12}C and ^{184}W ³⁾. Since the reachable range of the Ξ^- hyperon vacuum momenta at the considered photon energies is about of 0.2–2.5 GeV/c (see below), one needs to evaluate it also for such in-medium Ξ^- momenta at saturation

¹⁾This potential for the chosen in the present work ratio $\langle \rho_N \rangle / \rho_0$ of 0.55 and 0.76 for ^{12}C and ^{184}W nuclei of interest for positively and negatively charged hadrons is about of +3.6 and +17.3 MeV and -3.6 and -17.3 MeV for these nuclei, respectively.

²⁾Since the incident photons interact with the intranuclear nucleons practically in the whole volume of the nucleus due to the lack of strong initial-state interactions.

³⁾It should be pointed out that this assumes a purely isoscalar Ξ^- potential $U_{\Xi^-}^{\text{isoscalar}}(r)$, associated with the total nuclear density $\rho_n(r) + \rho_p(r)$, for both these nuclei and does not take into account the contribution to the total strong nuclear Ξ^- potential $U_{\Xi^-}(r)$ from the isovector one $U_{\Xi^-}^{\text{isovector}}(r)$, appearing in the neutron-rich nuclei due to the neutron excess density $\rho_n(r) - \rho_p(r)$. The latter might be nonnegligible in the ^{184}W nucleus. As was shown in Ref. [33], the ratio $U_{\Xi^-}^{\text{isovector}}(r)/U_{\Xi^-}^{\text{isoscalar}}(r)$ for this nucleus can reach the value of -0.5, which is nonnegligible. The above-mentioned means that a more realistic analysis of the Ξ^- hyperon production in heavy asymmetric targets should take into account in principle not only the isoscalar Ξ^- -nucleus potential, but also and an isovector one. However, since the main difference between the Ξ^- nuclear potentials in light (symmetric) and heavy (asymmetric) nuclei is coming from the Coulomb forces, which are included in our model, one may hope that the role played by the real isovector Ξ^- potential in this production will be moderate. Its rigorous evaluation is beyond the scope of the present study.

density ρ_0 . In line with the light quark content of the Ξ^- hyperons: $\Xi^- = |dss\rangle$, their mean-field scalar $U_{S\Xi^-}$ and vector $U_{V\Xi^-}$ potentials are about 1/3 of those U_{SN} and U_{VN} of a nucleon [43–45] when in-medium nucleon and Ξ^- hyperon velocities v'_N and v'_{Ξ^-} with respect to the surrounding nuclear matter are equal to each other, i.e.,

$$U_{S\Xi^-}(v'_{\Xi^-}, \rho_N) = \frac{1}{3}U_{SN}(v'_N, \rho_N),$$

$$U_{V\Xi^-}(v'_{\Xi^-}, \rho_N) = \frac{1}{3}\alpha U_{VN}(v'_N, \rho_N); \quad v'_N = v'_{\Xi^-}. \quad (4)$$

The condition that velocities v'_N and v'_{Ξ^-} are equal to each other leads to the following relation between the in-medium nucleon p'_N and the Ξ^- hyperon p'_{Ξ^-} momenta:

$$p'_N = \frac{\langle m_N^* \rangle}{\langle m_{\Xi^-}^* \rangle} p'_{\Xi^-}. \quad (5)$$

But, to simplify the calculations of the Ξ^- -nucleus single-particle potential (or the so-called Schrödinger equivalent potential $V_{\Xi^-A}^{\text{SEP}}$), we will use in Eq. (5) vacuum nucleon and Ξ^- hyperon masses m_N and m_{Ξ^-} instead of their average in-medium masses $\langle m_N^* \rangle$ and $\langle m_{\Xi^-}^* \rangle$. Then, this potential $V_{\Xi^-A}^{\text{SEP}}$ is derived from the Ξ^- in-medium energy as [44, 45]:

$$V_{\Xi^-A}^{\text{SEP}}(p'_{\Xi^-}, \rho_N) = \sqrt{[m_{\Xi^-} + U_{S\Xi^-}(p'_{\Xi^-}, \rho_N)]^2 + (p'_{\Xi^-})^2} + U_{V\Xi^-}(p'_{\Xi^-}, \rho_N) - \sqrt{m_{\Xi^-}^2 + (p'_{\Xi^-})^2}. \quad (6)$$

The relation between the potentials U_{Ξ^-} and $V_{\Xi^-A}^{\text{SEP}}$ at density ρ_0 is given by

$$U_{\Xi^-}(p'_{\Xi^-}) = \frac{\sqrt{m_{\Xi^-}^2 + (p'_{\Xi^-})^2}}{m_{\Xi^-}} V_{\Xi^-A}^{\text{SEP}}(p'_{\Xi^-}). \quad (7)$$

Adopting the following parametrizations for the nucleon potentials U_{SN} and U_{VN} at density ρ_0 from [46]

$$U_{SN}(p'_N, \rho_0) = -\frac{494.2272}{1 + 0.3426\sqrt{p'_N/p_F}} \text{ MeV}, \quad (8)$$

$$U_{VN}(p'_N, \rho_0) = \frac{420.5226}{1 + 0.4585\sqrt{p'_N/p_F}} \text{ MeV} \quad (9)$$

(where $p_F = 1.35 \text{ fm}^{-1} = 0.2673 \text{ GeV}/c$), we calculated, with accounting for Eqs. (4)–(7) as well as by multiplying the vector nucleon potential in Eq. (4) by a factor α of $\alpha = 1.068$ [42] to get for Λ hyperon potential $V_{\Lambda A}^{\text{SEP}}$ at zero momentum and at density ρ_0 an experimental value of $-(32 \pm 2)$ MeV [47], the momentum dependences of potentials $V_{\Xi^-A}^{\text{SEP}}$ and U_{Ξ^-} at saturation density. The Ξ^- potentials $V_{\Xi^-A}^{\text{SEP}}$ and U_{Ξ^-} , adjusted in this way, are shown in Fig. 1 by dashed and dotted-dotted-dashed curves, respectively. It is seen that these potentials are attractive for all momenta below of about 0.9 GeV/c with the value of $V_{\Xi^-A}^{\text{SEP}}(0) = U_{\Xi^-}(0) \approx -15$ MeV, whereas they are repulsive for higher momenta and increase monotonically with the growth of Ξ^- momentum. This value is in good agreement with the Ξ^- -nucleus potential depths of about -16 and -14 MeV, inferred from the analysis of the data on the missing-mass spectra for the $^{12}\text{C}(K^-, K^+)$ reaction in the Ξ^- -bound state region collected by the KEK-PS E224 [10] and BNL-AGS E885 [11] Collaborations at initial momenta of 1.6 and 1.8 GeV/c, correspondingly. Furthermore, it is also well consistent with that of ≈ -16 MeV for the in-medium Ξ^- mass shift predicted recently in Ref. [48] in the framework of the chiral soliton model. In addition, results for two Ξ^- potentials $V_{\Xi^-A}^{\text{SEP}}$, U_{Ξ^-} , obtained by multiplying the vector nucleon potential in Eq. (4) by factors α of $\alpha = 1.08995$ and $\alpha = 1.0019$ to get for the Ξ^- hyperon single-particle potential $V_{\Xi^-A}^{\text{SEP}}$ at zero momentum and at density ρ_0 the values of -11.96 and

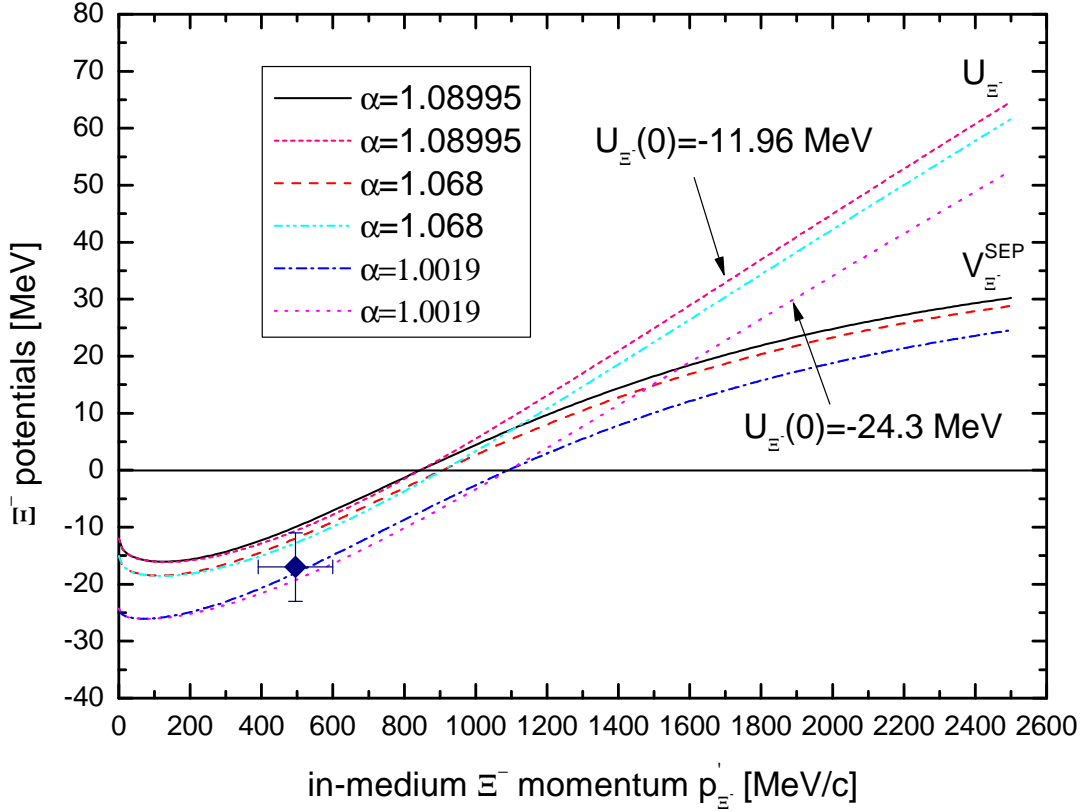


Figure 1: (Color online) Momentum dependence of the Schrödinger equivalent and effective scalar Ξ^- hyperon potentials at density ρ_0 . For notation see the text.

-24.3 MeV, are given in Fig. 1 as well. These values were deduced very recently in Refs. [8] and [9], correspondingly, from the analysis of the Ξ^- capture events in light nuclear emulsion identified in KEK and J-PARC experiments [5–7] within the quark mean-field model and in the framework of a $t\rho$ optical potential method. These potentials are depicted in Fig. 1 by solid, short-dashed and dotted-dashed, dotted lines, respectively. It is seen that now the former potentials are attractive at all momenta below of about 0.85 GeV/c, whereas they are repulsive at higher momenta. Contrary to this case, the latter potentials turn to repulsion at fairly high momenta, around 1.1 GeV/c. At momenta below ≈ 0.8 GeV/c these potentials, respectively, are more weakly and are more strongly attractive than those, calculated for a correction factor $\alpha = 1.068$. And they, correspondingly, are more strongly and are more weakly repulsive than the latters at Ξ^- momenta above ≈ 1.1 GeV/c. Since currently there are essential uncertainties in determining the Ξ^- nuclear potential both at threshold and at finite momenta below 1 GeV/c (cf. [23–31]), it is natural to adopt for certainty for the quantity U_{Ξ^-} in the present work two momentum dependences denoted in Fig. 1 by the short-dashed and dotted lines, respectively, and corresponding at zero momentum relative to the bulk matter to the values of $U_{\Xi^-}(0) = -11.96$ MeV and $U_{\Xi^-}(0) = -24.3$ MeV. This will allow us to explore the sensitivity of the Ξ^- production cross sections from the direct processes (1), (2) to the potential U_{Ξ^-} . Moreover, to extend the range of applicability of our model, we will also ignore it in our calculations. Thus, the results will be given for three scenarios for a Ξ^- potential: i) momentum-dependent potential with a value of $U_{\Xi^-}(0) = -24.3$ MeV, ii) momentum-dependent

potential with a value of $U_{\Xi^-}(0) = -11.96$ MeV and iii) zero potential at all Ξ^- momenta, achievable in the Ξ^- production in γA interactions at photon energies of interest. It should be pointed out that nowadays there is no experimental information about the momentum dependence of the Ξ^- nuclear potential at finite momenta. To some extent, such "experimental" information on the possible strength of the Ξ^- nuclear potential for Ξ^- - ^8Li system for finite momenta follows from the analysis [17] of the BNL-E906 measurement [14] of the spectrum of the $^9\text{Be}(K^-, K^+)$ reaction at initial K^- momentum of 1.8 GeV/c in the Ξ^- quasi-free region within the DWIA method. The strength of (-17 ± 6) MeV for this potential, taken in the Woods-Saxon form, was extracted from this analysis in the momentum transfer region $q \simeq 390$ – 600 MeV/c [17]. If we suppose that $p'_{\Xi^-} = q$, then this value, shown as data point in Fig. 1, can be considered as the central depth of the Ξ^- -nucleus potential in the momentum range of $\simeq 390$ – 600 MeV/c and, therefore, it can be compared with the aforementioned predictions given in this figure. One can see that only calculation, which corresponds to $V_{\Xi^-A}^{\text{SEP}}(0) = -24.3$ MeV, is fairly consistent with the result of [17] over the momentum range of 390–600 MeV/c. More detailed information on the Ξ^- potential at finite momenta could be in particular obtained from comparison the results of the present model calculations with the respective precise experimental data on direct Ξ^- photoproduction on nuclei. These data could be collected in future dedicated experiment at the CEBAF facility using high-intensity photon beams.

The total energy E'_h of the hadron in nuclear medium is linked with its average effective mass $\langle m_h^* \rangle$ and its in-medium momentum \mathbf{p}'_h as follows [33, 38]:

$$E'_h = \sqrt{(\mathbf{p}'_h)^2 + (\langle m_h^* \rangle)^2}. \quad (10)$$

The hadron in-medium momentum \mathbf{p}'_h is related to its vacuum momentum \mathbf{p}_h in the following way [33, 38]:

$$E'_h = \sqrt{(\mathbf{p}'_h)^2 + (\langle m_h^* \rangle)^2} = \sqrt{\mathbf{p}_h^2 + m_h^2} = E_h, \quad (11)$$

where E_h is the hadron total energy in vacuum. For the considered above Ξ^- hyperon momentum-dependent potentials its in-medium momentum p'_{Ξ^-} , with accounting for the relation (3), is the root of an equation (11) at given vacuum momentum p_{Ξ^-} . This root can be found by using the respective numerical procedure. But, to simplify the calculation of the Ξ^- production in γA interactions, we will determine these potentials at Ξ^- hyperon vacuum momentum p_{Ξ^-} and after that, employing Eq. (11), its in-medium momentum p'_{Ξ^-} . For our aims, as we checked, this is well justified.

The Ξ^- hyperon–nucleon elastic cross section $\sigma_{\Xi^-N}^{\text{el}}$ is expected to be ~ 10 mb in the Ξ^- momentum range of 0.2–2.5 GeV/c [28, 29, 31, 49–53] studied in the present work. Its mean "free" path $\lambda_{\Xi^-}^{\text{el}}$ up to elastic scattering inside the nucleus, defined as $\lambda_{\Xi^-}^{\text{el}} = 1/(\langle \rho_N \rangle \sigma_{\Xi^-N}^{\text{el}})$, for this cross section and for average nucleon densities of $\langle \rho_N \rangle = 0.55\rho_0$ (^{12}C) and $\langle \rho_N \rangle = 0.76\rho_0$ (^{184}W), $\rho_0 = 0.16$ fm $^{-3}$ amounts ≈ 11 fm for ^{12}C and ≈ 8 fm for ^{184}W . The radii of ^{12}C and ^{184}W , which are approximately 3 and 7.4 fm, are, respectively, less than these values. Therefore, we can ignore elastic Ξ^-N scatterings in the present study. Since in-medium threshold energies $\sqrt{s_{\text{th}}^*} = 2 \langle m_{K^+}^* \rangle + \langle m_{\Xi^-}^* \rangle$ and $\sqrt{s_{\text{th}}^*} = \langle m_{K^+}^* \rangle + \langle m_{K^0}^* \rangle + \langle m_{\Xi^-}^* \rangle$ of the elementary reactions (1) and (2) are practically equal to each other for both considered target nuclei and the free total cross sections of these reactions are also practically equal to each other [54] at beam energies of interest, we assume that their in-medium total cross sections are practically equal to each other as well. Then, neglecting the attenuation of the initial photon beam in the nuclear matter and describing the Ξ^- hyperon final-state absorption by the in-medium total inelastic Ξ^-N cross section $\sigma_{\Xi^-N}^{\text{in}}(p'_{\Xi^-})$, we express the inclusive differential cross section for direct production of Ξ^- hyperons off nuclei in the processes (1), (2) as [55]:

$$\frac{d\sigma_{\gamma A \rightarrow \Xi^- X}^{\text{(dir)}}(E_\gamma, \mathbf{p}_{\Xi^-})}{d\mathbf{p}_{\Xi^-}} = I_V[A] \left\langle \frac{d\sigma_{\gamma p \rightarrow K^+ K^+ \Xi^-}(\mathbf{p}_\gamma, \mathbf{p}'_{\Xi^-})}{d\mathbf{p}'_{\Xi^-}} \right\rangle_A \frac{d\mathbf{p}'_{\Xi^-}}{d\mathbf{p}_{\Xi^-}}, \quad (12)$$

where

$$I_V[A] = 2\pi A \int_0^R r_\perp dr_\perp \int_{-\sqrt{R^2-r_\perp^2}}^{\sqrt{R^2-r_\perp^2}} dz \rho(\sqrt{r_\perp^2+z^2}) \exp \left[-\sigma_{\Xi^-N}^{\text{in}}(p'_{\Xi^-}) A \int_z^{\sqrt{R^2-r_\perp^2}} \rho(\sqrt{r_\perp^2+x^2}) dx \right]; \quad (13)$$

$$\sigma_{\Xi^-N}^{\text{in}}(p'_{\Xi^-}) = \frac{Z}{A} \sigma_{\Xi^-p}^{\text{in}}(p'_{\Xi^-}) + \frac{N}{A} \sigma_{\Xi^-n}^{\text{in}}(p'_{\Xi^-}) \quad (14)$$

and

$$\left\langle \frac{d\sigma_{\gamma p \rightarrow K^+K^+\Xi^-}(\mathbf{p}_\gamma, \mathbf{p}'_{\Xi^-})}{d\mathbf{p}'_{\Xi^-}} \right\rangle_A = \int \int P_A(\mathbf{p}_t, E) d\mathbf{p}_t dE \quad (15)$$

$$\times \left\{ \frac{d\sigma_{\gamma p \rightarrow K^+K^+\Xi^-}[\sqrt{s^*}, \langle m_{K^+}^* \rangle, \langle m_{K^+}^* \rangle, \langle m_{\Xi^-}^* \rangle, \mathbf{p}'_{\Xi^-}]}{d\mathbf{p}'_{\Xi^-}} \right\}, \quad (16)$$

$$s^* = (E_\gamma + E_t)^2 - (\mathbf{p}_\gamma + \mathbf{p}_t)^2, \quad (16)$$

$$E_t = M_A - \sqrt{(-\mathbf{p}_t)^2 + (M_A - m_N + E)^2}. \quad (17)$$

Here, $d\sigma_{\gamma p \rightarrow K^+K^+\Xi^-}[\sqrt{s^*}, \langle m_{K^+}^* \rangle, \langle m_{K^+}^* \rangle, \langle m_{\Xi^-}^* \rangle, \mathbf{p}'_{\Xi^-}]/d\mathbf{p}'_{\Xi^-}$ is the in-medium differential cross section for the production of Ξ^- hyperon with modified mass $\langle m_{\Xi^-}^* \rangle$ and in-medium momentum \mathbf{p}'_{Ξ^-} in process (1) at the γp center-of-mass energy $\sqrt{s^*}$. The K^+ mesons are produced in this process with the medium modified mass $\langle m_{K^+}^* \rangle$ as well. E_γ and \mathbf{p}_γ are the total energy and momentum of the incident photon; $\rho(\mathbf{r})$ and $P_A(\mathbf{p}_t, E)$ are the local nucleon density and the spectral function of the target nucleus A normalized to unity (the information about these quantities can be found in Refs. [39, 56–58]); \mathbf{p}_t and E are the momentum and removal energy of the struck target proton participating in the production process (1); Z and N are the numbers of protons and neutrons in the target nucleus ($A = Z + N$), M_A and R are its mass and radius; m_N is the bare nucleon mass. In Eq. (12) we assume that the Ξ^- production cross sections in γp and γn reactions (1) and (2) are the same [54] as well as that the way of the produced Ξ^- hyperon from the production point in the nucleus to a free space is not perturbed by a relatively weak nuclear fields being considered in the present work, by the attractive Coulomb potential and by rare Ξ^-N elastic scatterings. Therefore, the in-medium hyperon momentum \mathbf{p}'_{Ξ^-} is assumed to be parallel to the vacuum one \mathbf{p}_{Ξ^-} and they are related by the Eq. (11).

According to [33, 38], we assume that the differential cross section $d\sigma_{\gamma p \rightarrow K^+K^+\Xi^-}[\sqrt{s^*}, \langle m_{K^+}^* \rangle, \langle m_{K^+}^* \rangle, \langle m_{\Xi^-}^* \rangle, \mathbf{p}'_{\Xi^-}]/d\mathbf{p}'_{\Xi^-}$ for Ξ^- hyperon production via reaction (1) in a nuclear medium is equivalent to the respective free space cross section calculated for the off-shell kinematics of this reaction and for the final K^+ mesons and Ξ^- hyperon in-medium masses $\langle m_{K^+}^* \rangle$ and $\langle m_{\Xi^-}^* \rangle$. In our calculations, this differential cross section has been described according to the three-body phase space at beam energies of interest (cf. [35]⁴):

$$\frac{d\sigma_{\gamma p \rightarrow K^+K^+\Xi^-}[\sqrt{s^*}, \langle m_{K^+}^* \rangle, \langle m_{K^+}^* \rangle, \langle m_{\Xi^-}^* \rangle, \mathbf{p}'_{\Xi^-}]}{d\mathbf{p}'_{\Xi^-}} = \frac{\pi}{4} \quad (18)$$

$$\times \frac{\sigma_{\gamma p \rightarrow K^+K^+\Xi^-}(E_\gamma^*, E_\gamma^{\text{th}})}{I_3[s^*, \langle m_{K^+}^* \rangle, \langle m_{K^+}^* \rangle, \langle m_{\Xi^-}^* \rangle] E'_{\Xi^-}} \frac{\lambda[s_{K^+K^+}^*, (\langle m_{K^+}^* \rangle)^2, (\langle m_{K^+}^* \rangle)^2]}{s_{K^+K^+}^*},$$

where

$$I_3[s^*, a, b, c] = \left(\frac{\pi}{2}\right)^2 \int_{(b+c)^2}^{(\sqrt{s^*}-a)^2} \frac{\lambda[x, b^2, c^2]}{x} \frac{\lambda[s^*, x, a^2]}{s^*} dx, \quad (19)$$

⁴ Presented here experimental angular distributions of the Ξ^- and K^+ in the photon-proton center-of-mass frame show practically an isotropic behavior at photon energies below 3.0 GeV.

$$\lambda(x, y, z) = \sqrt{[x - (\sqrt{y} + \sqrt{z})^2][x - (\sqrt{y} - \sqrt{z})^2]}, \quad (20)$$

$$s_{K^+K^+}^* = s^* + (\langle m_{\Xi^-}^* \rangle)^2 - 2(E_\gamma + E_t)E_{\Xi^-}' + 2(\mathbf{p}_\gamma + \mathbf{p}_t)\mathbf{p}_{\Xi^-}', \quad (21)$$

and

$$E_\gamma^* = \frac{s^* - m_p^2}{2m_p}, \quad E_\gamma^{\text{th}} = \frac{s_{\text{th}}^* - m_p^2}{2m_p}. \quad (22)$$

Here, $\sigma_{\gamma p \rightarrow K^+K^+\Xi^-}(E_\gamma^*, E_\gamma^{\text{th}})$ is the in-medium total cross section of process (1). In line with the aforesaid, it is equivalent to the free cross section $\sigma_{\gamma p \rightarrow K^+K^+\Xi^-}(E_\gamma, E_\gamma^{\text{th}})$, in which the vacuum incident E_γ and threshold E_γ^{th} energies⁵⁾ are replaced by the in-medium ones E_γ^* and E_γ^{th} , defined by the Eq. (22).

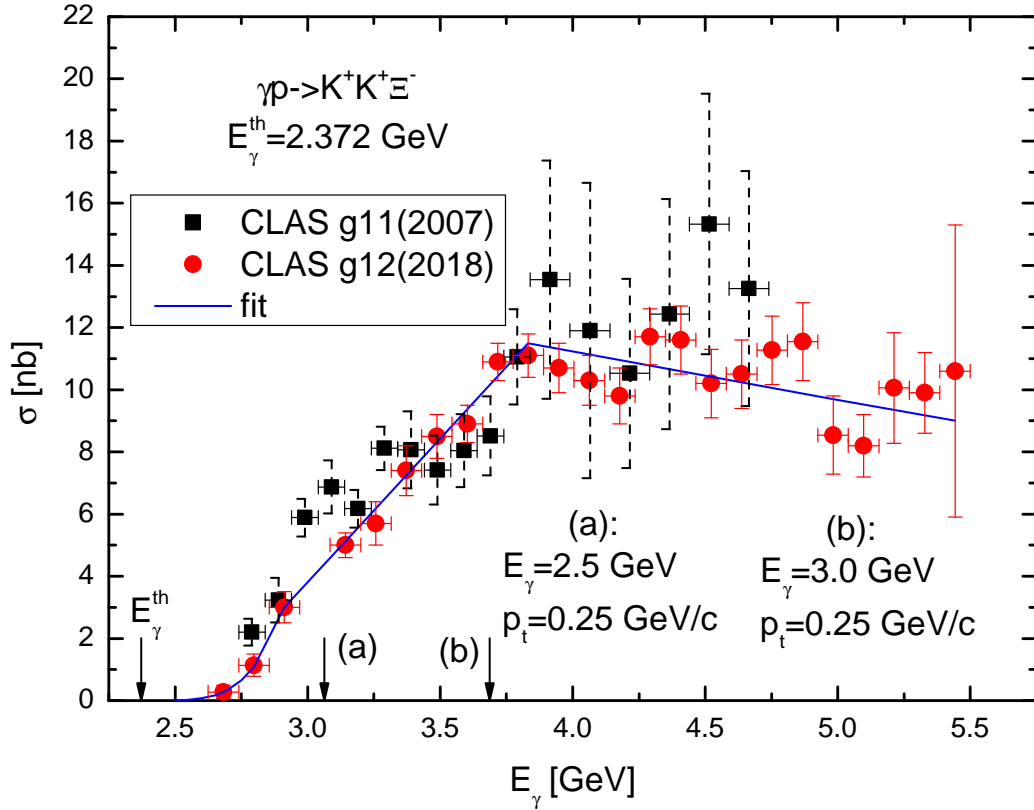


Figure 2: (Color online) Total cross section for the reaction $\gamma p \rightarrow K^+K^+\Xi^-$ as function of the incident photon energy E_γ . The left arrow indicates the free threshold energy for this reaction. The middle and right arrows indicate the effective photon energies $E_\gamma^* = 3.063$ GeV and $E_\gamma^* = 3.686$ GeV corresponding to the incident photon energies of 2.5 and 3.0 GeV, respectively, and a target proton bound in ^{12}C by 16 MeV and with momentum of 250 MeV/c. The latter one is directed opposite to the incoming photon beam. For the rest of the notation see the text.

The currently available experimental information on the free cross section $\sigma_{\gamma p \rightarrow K^+K^+\Xi^-}(E_\gamma, E_\gamma^{\text{th}})$ from CLAS g11 [35] and CLAS g12 [36] experiments, performed at Jefferson Lab in the photon

⁵⁾ Let us remind that $E_\gamma^{\text{th}} = 2.372$ GeV.

low-energy range $E_\gamma \leq 5.44$ GeV ⁶⁾, can be fitted as:

$$\sigma_{\gamma p \rightarrow K^+ K^+ \Xi^-}(E_\gamma, E_\gamma^{\text{th}}) \quad (23)$$

$$= \begin{cases} 41.733 [(E_\gamma - E_\gamma^{\text{th}})/\text{GeV}]^{4.278} \text{ [nb]} & \text{for } E_\gamma^{\text{th}} \leq E_\gamma \leq 2.9125 \text{ GeV,} \\ -23.909 + 9.239(E_\gamma/\text{GeV}) \text{ [nb]} & \text{for } 2.9125 \text{ GeV} < E_\gamma \leq 3.8325 \text{ GeV,} \\ 17.452 - 1.553(E_\gamma/\text{GeV}) \text{ [nb]} & \text{for } 3.8325 \text{ GeV} < E_\gamma \leq 5.4425 \text{ GeV.} \end{cases}$$

It is seen from Fig. 2 that the parametrization (23) (solid line) fits quite well the existing data [35, 36] (solid squares and circles). One can also see that the off-shell cross section $\sigma_{\gamma p \rightarrow K^+ K^+ \Xi^-}$, calculated in line with Eqs. (16), (17), (22) and (23) for photon energies of 2.5 and 3.0 GeV, a target proton bound in ^{12}C by 16 MeV, and with its internal momentum of 250 MeV/c directed opposite to the initial photon beam, is about 5 and 10 nb, respectively. This opens up the possibility of measuring the sizable Ξ^- hyperon production cross sections in (γ, Ξ^-) reactions near threshold at the CEBAF facility. It is worth noting that preliminary results for the total cross section of the reaction $\gamma p \rightarrow K^+ K^+ \Xi^-$ at higher photon energies have been recently obtained by the GlueX Collaboration at the upgraded up to 12 GeV CEBAF facility [37].

At the considered initial photon energies Ξ^- hyperons are mainly produced in γN interactions at small angles in the laboratory frame ⁷⁾. Therefore, we will calculate the Ξ^- momentum differential distributions from ^{12}C and ^{184}W target nuclei for the laboratory solid angle $\Delta\Omega_{\Xi^-} = 0^\circ \leq \theta_{\Xi^-} \leq 45^\circ$, and $0 \leq \varphi_{\Xi^-} \leq 2\pi$. Here, θ_{Ξ^-} is the polar angle of vacuum momentum \mathbf{p}_{Ξ^-} in the laboratory system with z-axis directed along the momentum \mathbf{p}_γ of the incident photon beam and φ_{Ξ^-} is the azimuthal angle of the Ξ^- momentum \mathbf{p}_{Ξ^-} in this system. We will require - as this has been done in Ref. [59] in the analysis of the data on η' meson photoproduction on ^{12}C target nucleus - that the produced with vacuum momentum \mathbf{p}_{Ξ^-} Ξ^- hyperon goes backward in the c.m.s. of the incident photon beam and a target nucleon at rest to guaranty that it will have relatively low momentum in the laboratory system, at which the sensitivity of the Ξ^- hyperon yield to its in-medium modification is expected to be enhanced, Then, accounting for Eq. (12), we can express the respective differential cross section for direct photon-induced Ξ^- hyperon production off nuclei from the processes (1), (2), corresponding to this solid angle and to this kinematical condition, in the form:

$$\frac{d\sigma_{\gamma A \rightarrow \Xi^- X}^{\text{(dir)}}(E_\gamma, p_{\Xi^-})}{dp_{\Xi^-}} = \int_{\Delta\Omega_{\Xi^-}} d\Omega_{\Xi^-} \frac{d\sigma_{\gamma A \rightarrow \Xi^- X}^{\text{(dir)}}(E_\gamma, \mathbf{p}_{\Xi^-})}{d\mathbf{p}_{\Xi^-}} p_{\Xi^-}^2 Q(\cos \theta_{\Xi^-}^{\text{cm}}) \quad (24)$$

$$= 2\pi \left(\frac{p_{\Xi^-}}{p'_{\Xi^-}} \right) I_V[A] \int_{\cos 45^\circ}^1 d \cos \theta_{\Xi^-} \left\langle \frac{d\sigma_{\gamma p \rightarrow K^+ K^+ \Xi^-}(p_\gamma, p'_{\Xi^-}, \theta_{\Xi^-})}{dp'_{\Xi^-} d\Omega_{\Xi^-}} \right\rangle_A Q(\cos \theta_{\Xi^-}^{\text{cm}}),$$

where the " Ξ^- c.m.s. forward emission eliminating" factor $Q(\cos \theta_{\Xi^-}^{\text{cm}})$ is defined in the following way:

$$Q(\cos \theta_{\Xi^-}^{\text{cm}}) = \begin{cases} 1 & \text{for } -1 \leq \cos \theta_{\Xi^-}^{\text{cm}} < 0, \\ 0 & \text{otherwise} \end{cases} \quad (25)$$

and

$$\cos \theta_{\Xi^-}^{\text{cm}} = \frac{p_\gamma p_{\Xi^-} \cos \theta_{\Xi^-} - E_\gamma E_{\Xi^-} + E_\gamma^{\text{cm}} E_{\Xi^-}^{\text{cm}}}{p_\gamma^{\text{cm}} p_{\Xi^-}^{\text{cm}}}. \quad (26)$$

⁶⁾ The author thanks I. Strakovsky for sending this information from CLAS g11 experiment to him.

⁷⁾ For instance, the maximum angle of Ξ^- hyperon production off a free proton at rest in reaction (1) is about 20.3° at the photon energy of 3.0 GeV.

Here,

$$E_\gamma^{\text{cm}} = p_\gamma^{\text{cm}} = \frac{1}{2\sqrt{s}}\lambda(s, 0, m_p^2), \quad (27)$$

$$E_{\Xi^-}^{\text{cm}} = \gamma_{\text{cm}}(E_{\Xi^-} - p_{\Xi^-} v_{\text{cm}} \cos \theta_{\Xi^-}), \quad p_{\Xi^-}^{\text{cm}} = \sqrt{(E_{\Xi^-}^{\text{cm}})^2 - m_{\Xi^-}^2}, \quad (28)$$

$$\gamma_{\text{cm}} = (E_\gamma + m_p)/\sqrt{s}, \quad v_{\text{cm}} = p_\gamma/(E_\gamma + m_p), \quad s = (E_\gamma + m_p)^2 - p_\gamma^2. \quad (29)$$

In the following, we will present mainly the calculations based on the Eq. (24). For completeness and for seeing the role of introduced Ξ^- phase space limitations, we will also give below in Figs. 5, 6, 9, 10 the results of calculations, obtained assuming in this equation the "phase space eliminating" factor Q to equal to 1. They will be labeled here as "no limitations" case. We will also consider the impact of the Ξ^- modification in nuclear matter on the momentum dependence of such relative observable – the transparency ratio T_A defined as the ratio between the inclusive Ξ^- differential production cross section (24) on a heavy nucleus and a light one (^{12}C):

$$T_A(E_\gamma, p_{\Xi^-}) = \frac{12 d\sigma_{\gamma A \rightarrow \Xi^- X}^{(\text{dir})}(E_\gamma, p_{\Xi^-})/dp_{\Xi^-}}{A d\sigma_{\gamma C \rightarrow \Xi^- X}^{(\text{dir})}(E_\gamma, p_{\Xi^-})/dp_{\Xi^-}}. \quad (30)$$

For the total free inelastic $\Xi^- p$ and $\Xi^- n$ cross sections $\sigma_{\Xi^- p}^{\text{in}}$ and $\sigma_{\Xi^- n}^{\text{in}}$, which enter into Eq. (14) and which will be used in our calculations of Ξ^- production in γA reactions, in Ref. [33] the following laboratory Ξ^- momentum p_{Ξ^-} dependences have been suggested at Ξ^- momenta below 0.8 GeV/c

$$\sigma_{\Xi^- p}^{\text{in}}(p_{\Xi^-}) = \begin{cases} 2.417/(p_{\Xi^-})^{1.8106} \text{ [mb]} & \text{for } 0.15 \leq p_{\Xi^-} \leq 0.4 \text{ GeV/c,} \\ 12.7 \text{ [mb]} & \text{for } 0.4 < p_{\Xi^-} \leq 0.8 \text{ GeV/c,} \end{cases} \quad (31)$$

where momentum p_{Ξ^-} is expressed in GeV/c. And

$$\sigma_{\Xi^- n}^{\text{in}}(p_{\Xi^-}) = 23.448 \left(\sqrt{s_{\Xi^-}(p_{\Xi^-})} - \sqrt{s_0} \right)^{0.353} \text{ [mb]}. \quad (32)$$

Here,

$$s_{\Xi^-}(p_{\Xi^-}) = (E_{\Xi^-} + m_N)^2 - p_{\Xi^-}^2 \quad (33)$$

and $\sqrt{s_0} = m_\Lambda + m_{\Sigma^-} = 2.313132$ GeV is the free threshold energy for the $\Xi^- n \rightarrow \Lambda \Sigma^-$ reaction. For the in-medium $\Xi^- p$ and $\Xi^- n$ inelastic cross sections we adopt Eqs. (31) and (32), in which one needs to make only the substitution $p_{\Xi^-} \rightarrow p'_{\Xi^-}$. We extend the application of the above dependences to higher Ξ^- momenta of present interest since they fulfill available scarce experimental constraints [60] on the $\Xi^- N$ inelastic cross section at these momenta (cf. [61]). It is interesting to note that, as is easy to see, the integral (13) for the quantity $I_V[A]$ can be transformed to a simpler expression:

$$I_V[A] = \frac{\pi}{\sigma_{\Xi^- N}^{\text{in}}(p'_{\Xi^-})} \int_0^{R^2} dr_\perp^2 \left(1 - e^{-A \sigma_{\Xi^- N}^{\text{in}}(p'_{\Xi^-}) \frac{\int_{-\sqrt{R^2-r_\perp^2}}^{\sqrt{R^2-r_\perp^2}} \rho(\sqrt{r_\perp^2+x^2}) dx}{-\sqrt{R^2-r_\perp^2}}} \right), \quad (34)$$

which in the cases of Gaussian nuclear density ($\rho(\mathbf{r}) = (b/\pi)^{3/2} \exp(-br^2)$) and a uniform nucleon density for a nucleus of a radius $R = r_0 A^{1/3}$ with a sharp boundary is reduced to even more simple forms:

$$I_V[A] = \frac{A}{x_G} \int_0^1 \frac{dt}{t} \left(1 - e^{-x_G t} \right), \quad x_G = A \sigma_{\Xi^- N}^{\text{in}}(p'_{\Xi^-}) b/\pi \quad (35)$$

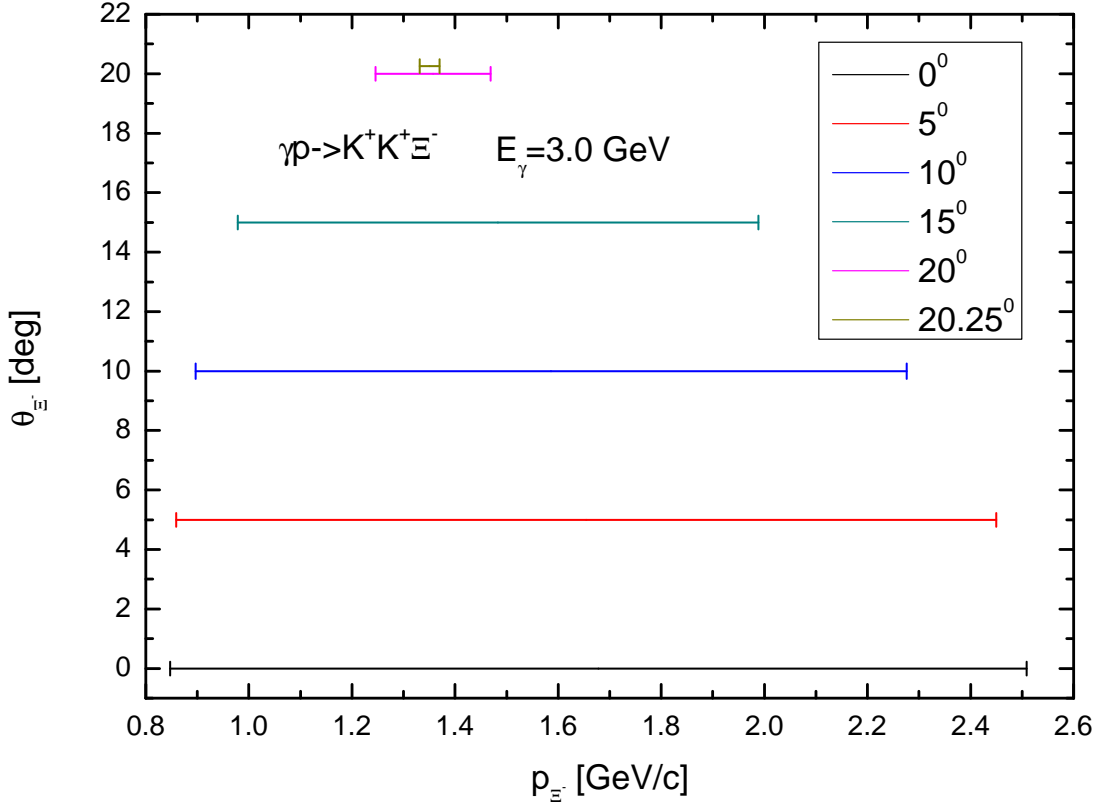


Figure 3: (Color online) The kinematically allowed momenta of Ξ^- hyperons in the laboratory frame in the reaction $\gamma p \rightarrow K^+ K^+ \Xi^-$ at polar angles, indicated in the inset, for an incident photon energy of 3.0 GeV. The target proton is free and at rest.

and

$$I_V[A] = \frac{3A}{2a_1} \left\{ 1 - \frac{2}{a_1^2} [1 - (1 + a_1)e^{-a_1}] \right\}, \quad a_1 = 3A\sigma_{\Xi^- N}^{\text{in}}(p'_{\Xi^-})/2\pi R^2, \quad (36)$$

respectively. The simple formulas (35) and (36) allow one to easily estimate the differential cross section (12) at above threshold energies.

Before closing this section, let us more closely consider, using the relativistic kinematics, more simpler case of the production of Ξ^- hyperons in the elementary reaction $\gamma p \rightarrow K^+ K^+ \Xi^-$ proceeding on a free target proton being at rest. This will help us to get some feeling about their kinematic characteristics allowed in this reaction at incident photon energies of interest. The differential cross section $d\sigma_{\gamma p \rightarrow K^+ K^+ \Xi^-}[\sqrt{s}, m_{K^+}, m_{K^+}, m_{\Xi^-}, \mathbf{p}_{\Xi^-}]/d\mathbf{p}_{\Xi^-}$ of this reaction can be obtained from more general one (18) in the limits: $\mathbf{p}_t \rightarrow 0$, $E_t \rightarrow m_p$, $\langle m_{K^+}^* \rangle \rightarrow m_{K^+}$, $\langle m_{\Xi^-}^* \rangle \rightarrow m_{\Xi^-}$, $\mathbf{p}'_{\Xi^-} \rightarrow \mathbf{p}_{\Xi^-}$, $E'_{\Xi^-} \rightarrow E_{\Xi^-}$, $E_\gamma^* \rightarrow E_\gamma$, $E_\gamma^{\text{th}} \rightarrow E_\gamma^{\text{th}}$, $s^* \rightarrow s$ and $s_{K^+ K^+}^* \rightarrow s_{K^+ K^+}$. The quantity $s_{K^+ K^+}$, entering into it, must be greater than or equal to $4m_{K^+}^2$. When the velocity v_{cm} of the γp center-of-mass system in the laboratory frame is greater than or equal to the maximal Ξ^- hyperon velocity $v_{\Xi^-}^{*\text{max}}$ in this system ($v_{\text{cm}} \geq v_{\Xi^-}^{*\text{max}}$), the condition $s_{K^+ K^+} \geq 4m_{K^+}^2$ leads to the fact that the polar Ξ^- production angle θ_{Ξ^-} in this frame ranges from 0 to a maximal value $\theta_{\Xi^-}^{\text{max}} = \arcsin[p_{\Xi^-}^{*\text{max}}/(\gamma_{\text{cm}} v_{\text{cm}} m_{\Xi^-})]$. Taking into account that the velocity $v_{\Xi^-}^{*\text{max}}$ can be expressed

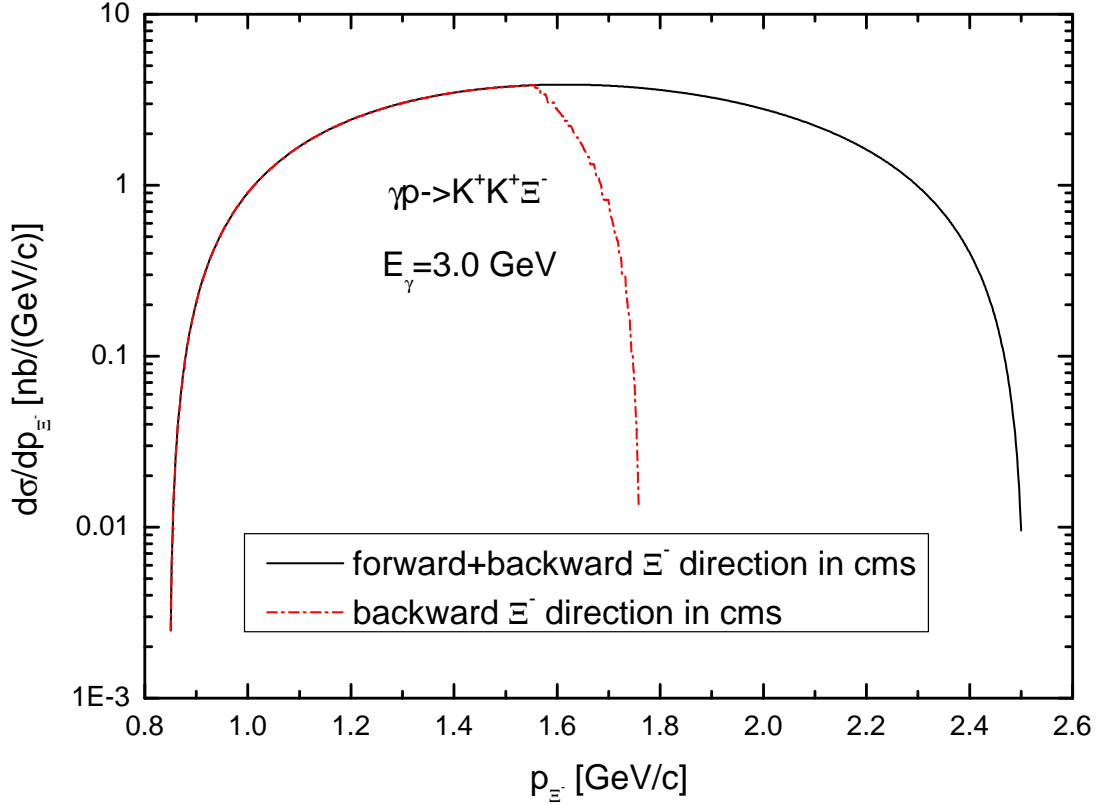


Figure 4: (Color online) Ξ^- momentum spectrum of the reaction $\gamma p \rightarrow K^+K^+\Xi^-$ in the full available laboratory polar angular range at an incident photon energy of 3.0 GeV, corresponding to the emission of Ξ^- in the forward+backward (solid curve) and backward (dotted-dashed curve) directions in the center-of-mass system of the incident photon beam and a free target proton at rest.

via maximal Ξ^- hyperon momentum $p_{\Xi^-}^{*\max}$ and its maximal total energy $E_{\Xi^-}^{*\max}$ in the γp c.m.s. as

$$v_{\Xi^-}^{*\max} = p_{\Xi^-}^{*\max}/E_{\Xi^-}^{*\max}, \quad (37)$$

where

$$p_{\Xi^-}^{*\max} = \frac{1}{2\sqrt{s}}\lambda(s, m_{\Xi^-}^2, 4m_{K^+}^2), \quad E_{\Xi^-}^{*\max} = \sqrt{(p_{\Xi^-}^{*\max})^2 + m_{\Xi^-}^2}, \quad (38)$$

we get, for instance, that $v_{\text{cm}} = 0.762$, $v_{\Xi^-}^{*\max} = 0.377$ and, respectively, $\theta_{\Xi^-}^{\max} = 20.3^\circ$ at $E_\gamma = 3.0$ GeV (cf. footnote 7) given above). At this energy, the value of the Ξ^- hyperon total energy $E_{\Xi^-}(\theta_{\Xi^-}^{\max})$ in the l.s., corresponding to its maximal production angle $\theta_{\Xi^-}^{\max} = 20.3^\circ$ is equal to $E_{\Xi^-}(\theta_{\Xi^-}^{\max}) = \gamma_{\text{cm}}m_{\Xi^-}^2/E_{\Xi^-}^{*\max} = 1.89$ GeV. This energy corresponds to the Ξ^- momentum $p_{\Xi^-}(\theta_{\Xi^-}^{\max}) = 1.35$ GeV/c (cf. Fig. 3). In the case when $v_{\text{cm}} \geq v_{\Xi^-}^{*\max}$, as also follows from the condition $s_{K^+K^+} \geq 4m_{K^+}^2$, the laboratory Ξ^- hyperon momentum p_{Ξ^-} at given production angle θ_{Ξ^-} , belonging to the interval $[0, \arcsin[p_{\Xi^-}^{*\max}/(\gamma_{\text{cm}}v_{\text{cm}}m_{\Xi^-})]]$, varies within the range:

$$\frac{p_\gamma\sqrt{s}E_{\Xi^-}^{*\max}\cos\theta_{\Xi^-} - (E_\gamma + m_p)\sqrt{s}\sqrt{(p_{\Xi^-}^{*\max})^2 - \gamma_{\text{cm}}^2v_{\text{cm}}^2m_{\Xi^-}^2\sin^2\theta_{\Xi^-}}}{(E_\gamma + m_p)^2 - p_\gamma^2\cos^2\theta_{\Xi^-}} \leq \quad (39)$$

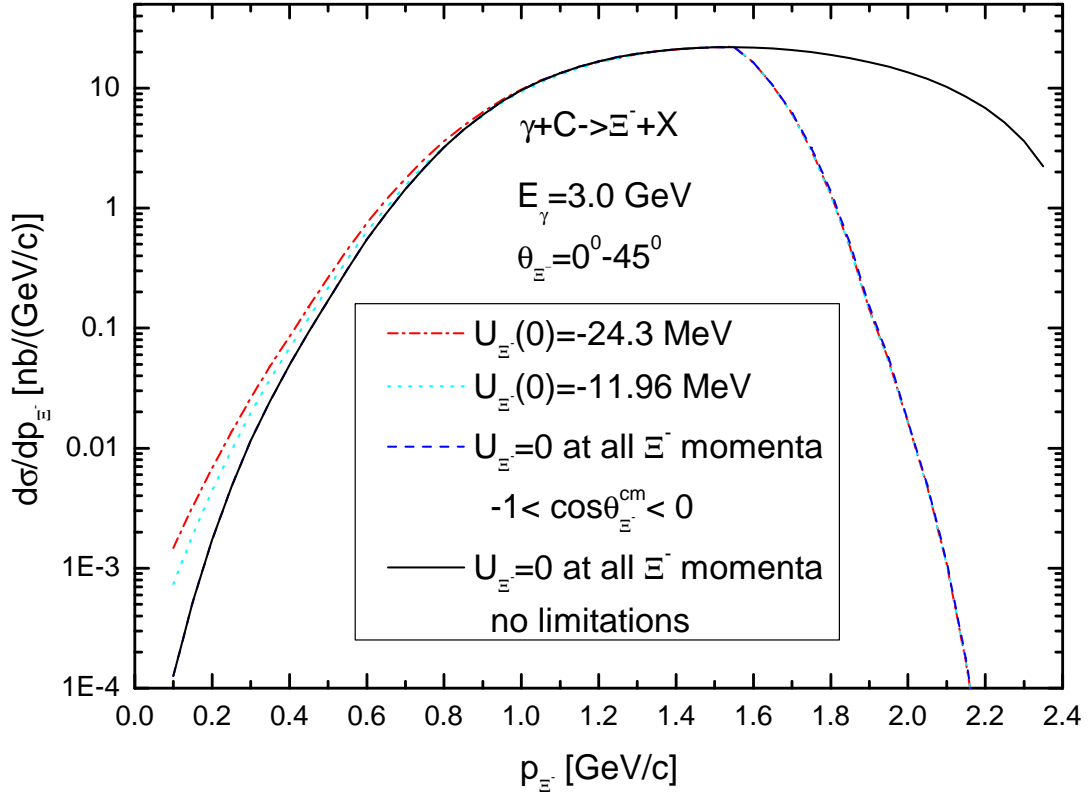


Figure 5: (Color online) Momentum differential cross sections for the production of Ξ^- hyperons from the direct $\gamma p \rightarrow K^+ K^+ \Xi^-$ and $\gamma n \rightarrow K^+ K^0 \Xi^-$ processes in the laboratory polar angular range of 0° – 45° in the interaction of photons of energy of 3.0 GeV with ^{12}C nucleus. They were calculated for two different momentum dependences of the Ξ^- hyperon effective scalar potential U_{Ξ^-} at density ρ_0 with the values $U_{\Xi^-}(0) = -24.3$ MeV and $U_{\Xi^-}(0) = -11.96$ MeV, presented in Fig. 1, for zero potential at all Ξ^- momenta, requiring that the Ξ^- hyperons go backwards in the center-of-mass system of the incident photon beam and a target nucleon at rest, as well as for zero potential at all Ξ^- momenta without any constraints on the Ξ^- emission angle in this system.

$$p_{\Xi^-} \leq \frac{p_\gamma \sqrt{s} E_{\Xi^-}^{*\max} \cos \theta_{\Xi^-} + (E_\gamma + m_p) \sqrt{s} \sqrt{(p_{\Xi^-}^{*\max})^2 - \gamma_{\text{cm}}^2 v_{\text{cm}}^2 m_{\Xi^-}^2 \sin^2 \theta_{\Xi^-}}}{(E_\gamma + m_p)^2 - p_\gamma^2 \cos^2 \theta_{\Xi^-}}.$$

In the case of zero Ξ^- production angle the expression (39) is reduced to the following more simpler form:

$$\gamma_{\text{cm}} E_{\Xi^-}^{*\max} (v_{\text{cm}} - v_{\Xi^-}^{*\max}) \leq p_{\Xi^-} \leq \gamma_{\text{cm}} E_{\Xi^-}^{*\max} (v_{\text{cm}} + v_{\Xi^-}^{*\max}). \quad (40)$$

The results of our calculations by (39), (40) for the kinematically allowed Ξ^- momenta in the laboratory system for the Ξ^- production angles of $0, 5, 10, 15, 20$ and 20.25° at $E_\gamma = 3.0$ GeV are given in Fig. 3. It is seen that, as the Ξ^- production angle increases, the kinematically allowed Ξ^- momentum range becomes narrower. Thus, for example, the laboratory Ξ^- hyperon momenta belong to the ranges of $0.85 \text{ GeV}/c \leq p_{\Xi^-} \leq 2.51 \text{ GeV}/c$, $0.98 \text{ GeV}/c \leq p_{\Xi^-} \leq 1.99 \text{ GeV}/c$ and $1.33 \text{ GeV}/c \leq p_{\Xi^-} \leq 1.37 \text{ GeV}/c$ at its production angles of $0, 15$ and 20.25° , respectively. The maximal momentum range is at zero Ξ^- production angle. Visual inspection of Fig. 3 tells us that

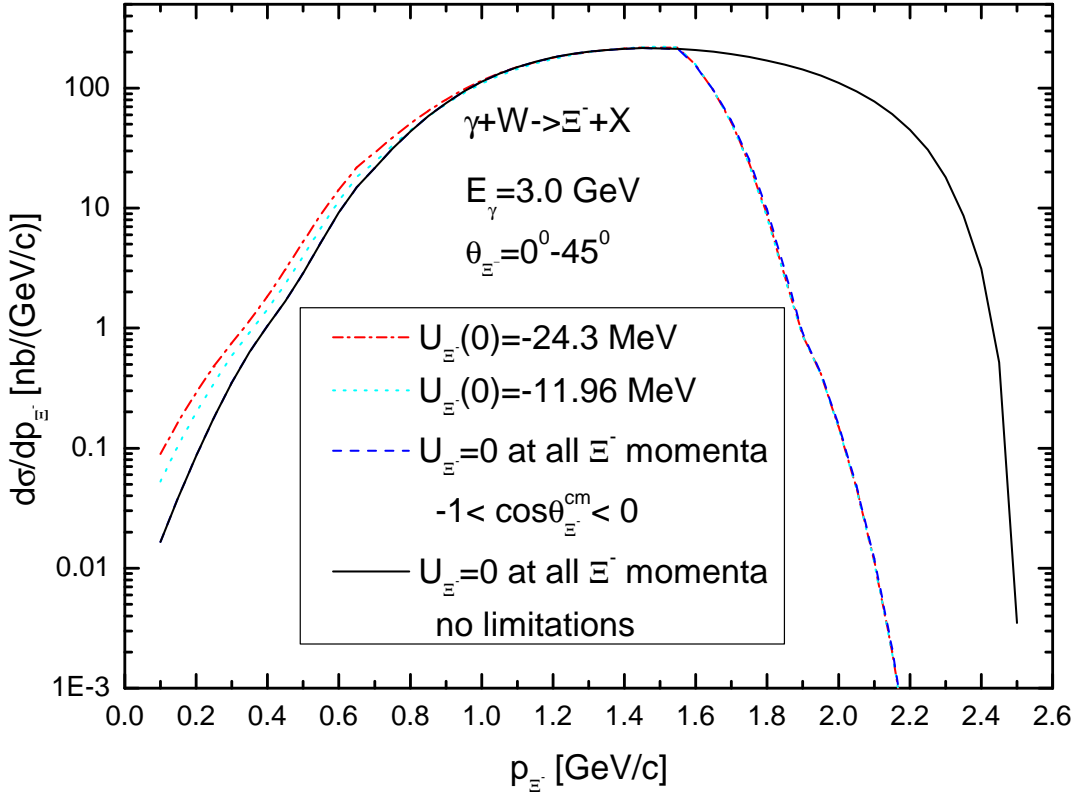


Figure 6: (Color online) The same as in Fig. 5, but for the W target nucleus.

for any given Ξ^- hyperon momentum p_{Ξ^-} from this range its laboratory production angle θ_{Ξ^-} varies within the limits:

$$0 \leq \theta_{\Xi^-} \leq \theta_{\Xi^-}^{\max}(p_{\Xi^-}) \leq \theta_{\Xi^-}^{\max}, \quad (41)$$

which corresponds to

$$\cos \theta_{\Xi^-}^{\max} \leq \cos \theta_{\Xi^-}^{\max}(p_{\Xi^-}) \leq \cos \theta_{\Xi^-} \leq 1. \quad (42)$$

The kinematical considerations show that

$$\cos \theta_{\Xi^-}^{\max}(p_{\Xi^-}) = (\gamma_{\text{cm}} E_{\Xi^-} - E_{\Xi^-}^{*\max}) / (\gamma_{\text{cm}} v_{\text{cm}} p_{\Xi^-}). \quad (43)$$

It is further interesting to calculate the Ξ^- momentum spectrum from the considered reaction $\gamma p \rightarrow K^+ K^+ \Xi^-$ in the cases when Ξ^- hyperons go only backwards and also backwards plus forwards in the γp c.m.s. When the Ξ^- momenta belong to the interval (40), we define this spectrum, in line with Eq. (24), as:

$$\frac{d\sigma_{\gamma p \rightarrow K^+ K^+ \Xi^-}(E_\gamma, p_{\Xi^-})}{dp_{\Xi^-}} = 2\pi \int_{\beta}^1 d \cos \theta_{\Xi^-} p_{\Xi^-}^2 \frac{d\sigma_{\gamma p \rightarrow K^+ K^+ \Xi^-}[\sqrt{s}, m_{K^+}, m_{K^+}, m_{\Xi^-}, \mathbf{p}_{\Xi^-}]}{d\mathbf{p}_{\Xi^-}} Q(\cos \theta_{\Xi^-}^{\text{cm}}), \quad (44)$$

where $\beta = \cos \theta_{\Xi^-}^{\max}(p_{\Xi^-})$ as well as in the former case the " Ξ^- phase space eliminating" factor Q is defined above by the Eq. (25) and in the latter case it is equal to 1. The results of calculations based

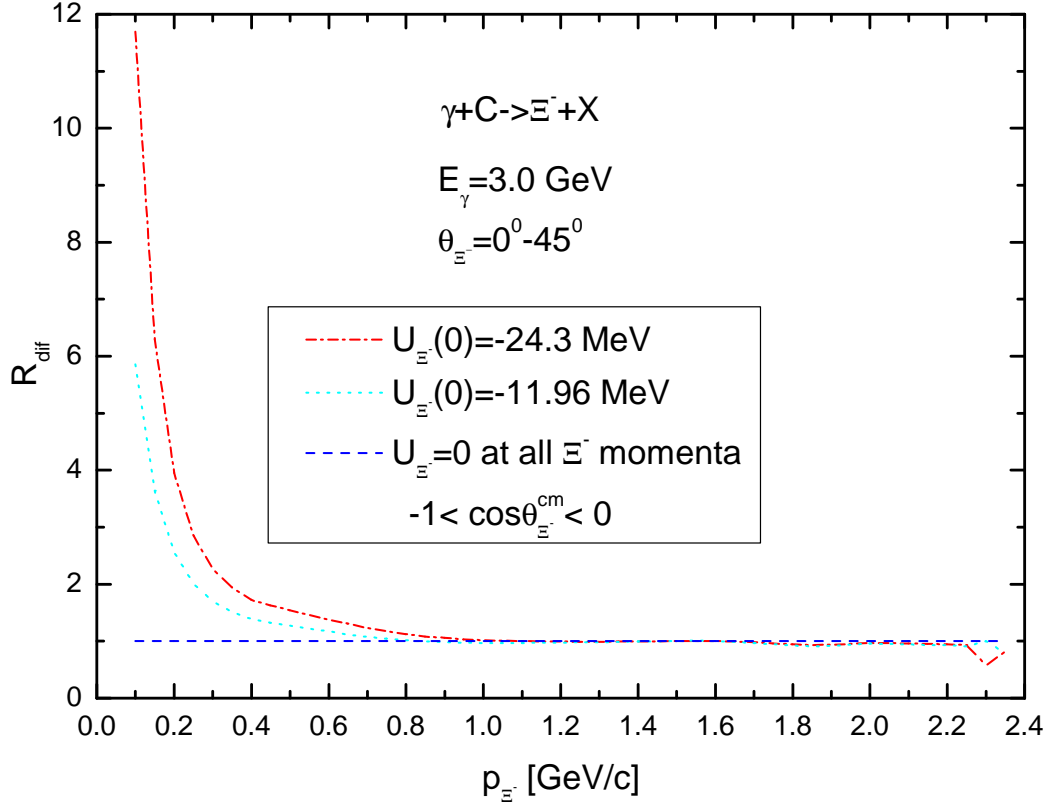


Figure 7: (Color online) Ratio between the differential cross sections for Ξ^- production on ^{12}C target nucleus in the angular region of 0° – 45° by photons of energy of 3.0 GeV, calculated for two different momentum dependences of the Ξ^- hyperon effective scalar potential U_{Ξ^-} at density ρ_0 with the values $U_{\Xi^-}(0) = -24.3$ MeV and $U_{\Xi^-}(0) = -11.96$ MeV and presented in Fig. 1 as well as for zero potential at all Ξ^- momenta and without this potential, requiring that the Ξ^- hyperons go backwards in the center-of-mass system of the incident photon beam and a target nucleus at rest, as a function of Ξ^- momentum.

on the Eq. (44) at $E_\gamma = 3.0$ GeV are presented in Fig. 4. It can be easily seen that when this factor is introduced, i.e. when only the backward c.m.s. Ξ^- momenta are allowed, the high-momentum tail of the full laboratory Ξ^- spectrum is suppressed and now the achievable Ξ^- momentum ranges from relatively high value of 0.85 GeV/c (cf. Fig. 3) to a sufficiently high one of ≈ 1.8 GeV/c. At such high Ξ^- momentum values it is difficult to expect the strong sensitivity of the Ξ^- hyperon yield from nuclei to its in-medium modifications. But if the Fermi motion and binding of the struck target proton are taken into account, a low-momentum tail of the Ξ^- momentum distribution from the considered elementary reaction appears. And this tail possesses already a definite sensitivity to these modifications (see below).

3 Results

The model described above makes it possible to calculate the absolute values of the differential cross sections for Ξ^- photoproduction off nuclei and their ratios. In the beginning, we consider

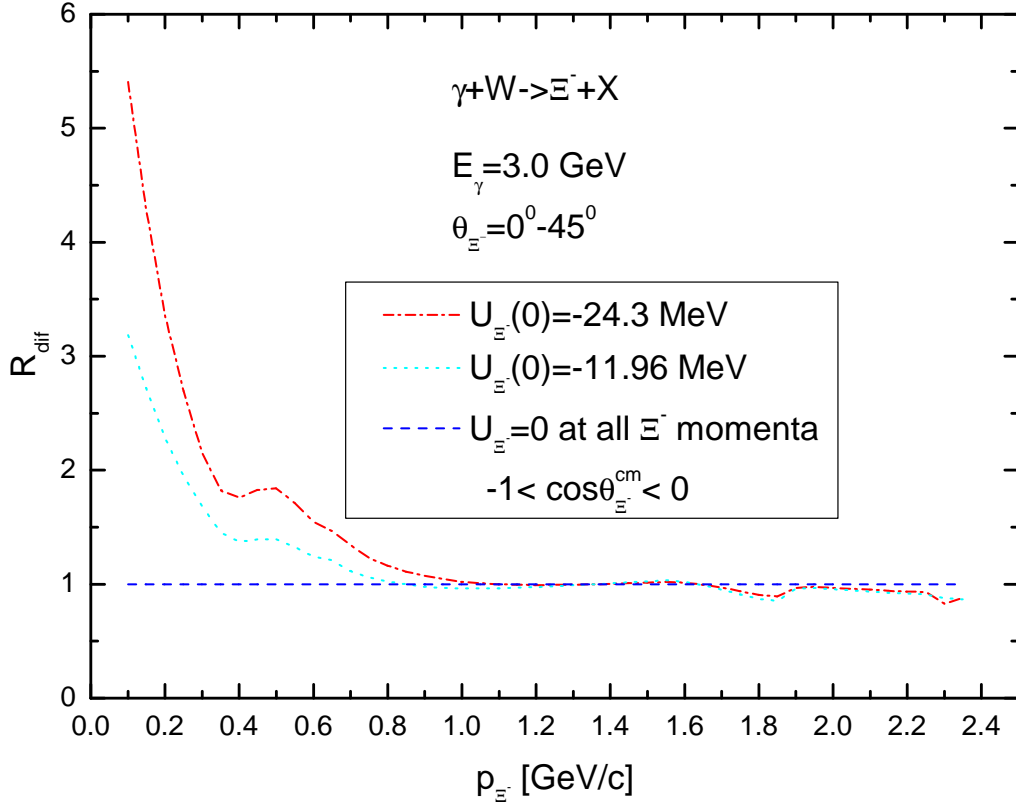


Figure 8: (Color online) The same as in Fig. 7, but for the W target nucleus.

the momentum dependences of these cross sections from the production channels (1) and (2) in $\gamma^{12}\text{C}$ and $\gamma^{184}\text{W}$ reactions. They were calculated in line with Eq. (24) for incident photon energy of 3.0 GeV within three employed scenarios for the Ξ^- effective scalar potential U_{Ξ^-} at density ρ_0 for laboratory polar angles of 0° – 45° with and without (“no limitations” case) imposing the phase space constraints on the Ξ^- emission angle in the γp c.m. system with a target proton being at rest. These dependences are shown, respectively, in Figs. 5 and 6. One can see from them that both the full Ξ^- hyperon momentum distributions (solid curves) and modified ones (dotted-dashed, dotted, dashed lines) possess a distinct sensitivity to changes in this potential in the low-momentum region of 0.1–0.8 GeV/c appearing, as was noted above, due to the binding of target nucleons and their Fermi motion for both target nuclei. Whereas, at higher Ξ^- momenta the impact of the Ξ^- potential on these distributions is negligible. In the low-momentum region, the differences between calculations corresponding to different options for the Ξ^- nuclear potential U_{Ξ^-} are well distinguishable and experimentally measurable. They are similar for both target nuclei at the considered photon energy of 3.0 GeV. Thus, for instance, for vacuum Ξ^- hyperon momenta of 0.2, 0.4, 0.6 GeV/c the inclusion of the Ξ^- momentum-dependent potential given above in Fig. 1 and having value of $U_{\Xi^-}(0) = -11.96$ MeV at density ρ_0 leads in the case of ^{12}C target nucleus to an enhancement of the Ξ^- production cross sections by factors of about 2.6, 1.4, 1.2, respectively, as compared to those obtained for these momenta in the scenario when potential $U_{\Xi^-} = 0$ MeV at all outgoing momenta. For the ^{184}W nucleus these enhancement factors are about 2.3, 1.4, 1.2. The inclusion of the Ξ^- attractive momentum-dependent potential with value of $U_{\Xi^-}(0) = -24.3$ MeV at

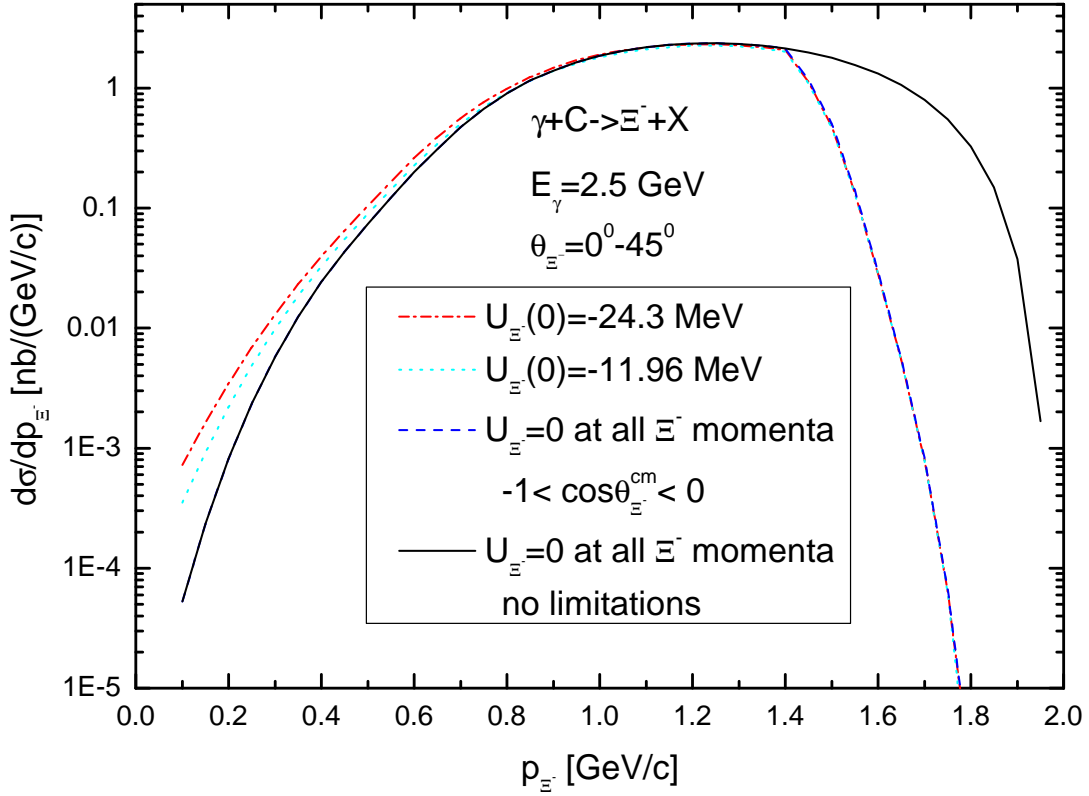


Figure 9: (Color online) Momentum differential cross sections for the production of Ξ^- hyperons from the direct $\gamma p \rightarrow K^+ K^+ \Xi^-$ and $\gamma n \rightarrow K^+ K^0 \Xi^-$ processes in the laboratory polar angular range of 0° – 45° in the interaction of photons of energy of 2.5 GeV with ^{12}C nucleus. They were calculated for two different momentum dependences of the Ξ^- hyperon effective scalar potential U_{Ξ^-} at density ρ_0 with the values $U_{\Xi^-}(0) = -24.3$ MeV and $U_{\Xi^-}(0) = -11.96$ MeV, presented in Fig. 1, for zero potential at all Ξ^- momenta, requiring that the Ξ^- hyperons go backwards in the center-of-mass system of the incident photon beam and a target nucleon at rest, as well as for zero potential at all Ξ^- momenta without any constraints on the Ξ^- emission angle in this system.

density ρ_0 results in the further enhancement of the Ξ^- hyperon production cross sections by factors of about 1.5, 1.2, 1.2 and 1.5, 1.3, 1.3 compared to those calculated for the above-mentioned Ξ^- momentum-dependent potential for the same outgoing vacuum Ξ^- momenta of 0.2, 0.4, 0.6 GeV/c in the cases of ^{12}C and ^{184}W target nuclei, respectively. The observed sensitivity of the strength of the low-momentum part of the Ξ^- spectrum on the scalar Ξ^- potential U_{Ξ^-} can be exploited to deduce the momentum dependence of this potential from the direct comparison of the shapes of the calculated Ξ^- hyperon differential distributions with that which could be determined in the dedicated experiment in the present experimental facilities (for example, at the CEBAF facility). Since the Ξ^- hyperon production differential cross sections on ^{12}C target nucleus are less than those on the ^{184}W by about of one to two orders of magnitude at all Ξ^- momenta, their measurements on a heavy nuclear targets like a tungsten one look quite promising and favorable. At the photon beam energy of 3.0 GeV and with imposing the considered kinematical constraints on the Ξ^- emission angle in the respective γp c.m.s. such measurements could be performed in a more narrower Ξ^-

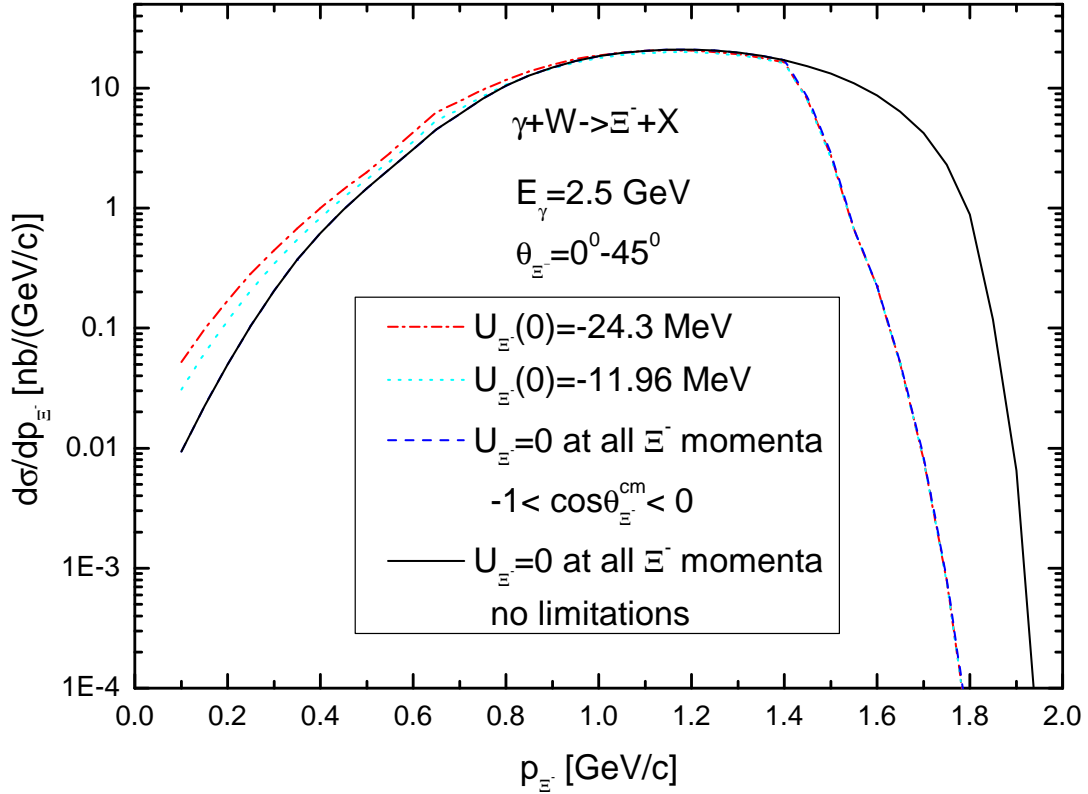


Figure 10: (Color online) The same as in Fig. 9, but for the W target nucleus.

momentum range compared to that, corresponding to the case when these constraints are ignored, for reliable determination of the Ξ^- nuclear potential.

The sensitivity of the differential distributions, given in Figs. 5 and 6, to the Ξ^- hyperon in-medium modification at the saturation density ρ_0 may be more clearly seen in the momentum dependences of the ratios R_{dif} of these distributions, calculated at incident photon energy of 3.0 GeV for two considered Ξ^- momentum-dependent potentials U_{Ξ^-} and for zero momentum-independent potential, to the analogous cross section, determined assuming that $U_{\Xi^-} = 0$ MeV at all Ξ^- momenta, with requiring that the Ξ^- hyperons go backwards in the center-of-mass system of the incident photon beam and a target nucleus at rest. We show in Figs. 7 and 8 such dependences on a linear scale for ^{12}C and ^{184}W nuclei, respectively. It should be emphasized that such relative observable is more preferred compared to that based on the absolute differential momentum distributions for the purpose of obtaining the definite information on particle in-medium properties, since the theoretical uncertainties associated with the description of the particle production on nuclei substantially cancel out in it. It is nicely seen from these figures that there are indeed experimentally measurable and similar differences for the Ξ^- momenta ≤ 0.8 GeV/c between the calculations corresponding to the adopted options for the scalar potential U_{Ξ^-} for both target nuclei. Whereas, at higher Ξ^- momenta these differences are practically indistinguishable.

We, therefore, come to the conclusion that the most interesting low-momentum in-medium properties of Ξ^- hyperons could be definitely studied via the momentum dependences of their absolute (and relative) production cross sections in inclusive photon-induced reactions at incident

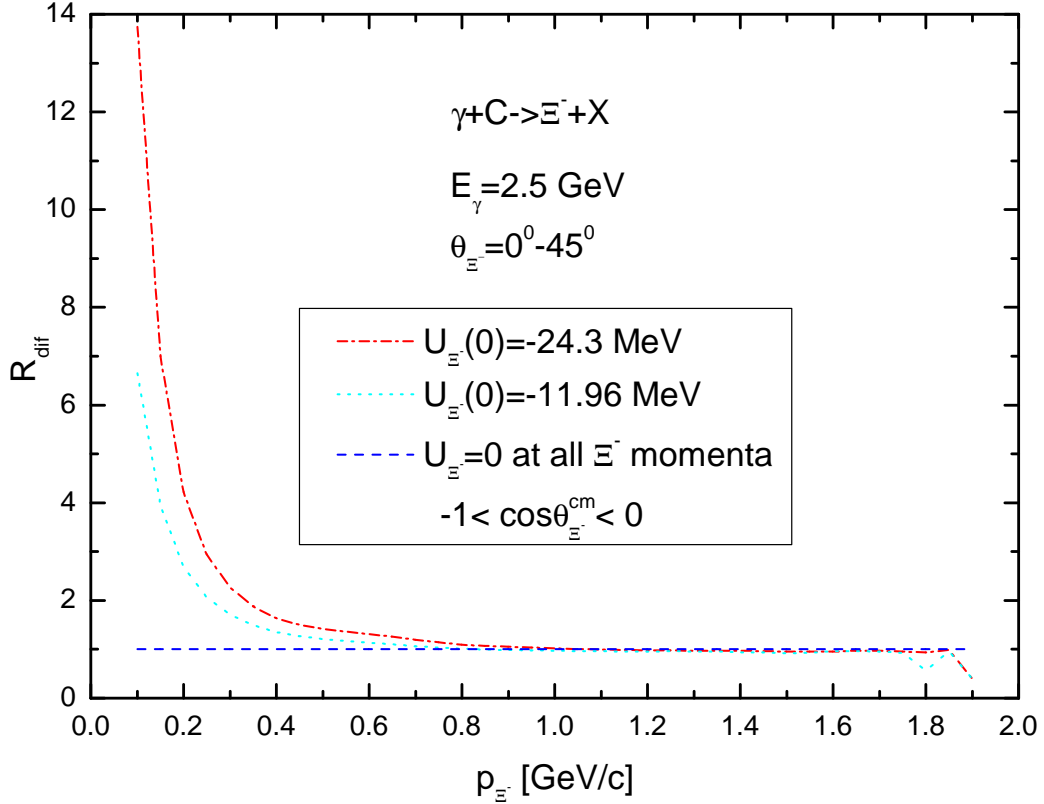


Figure 11: (Color online) Ratio between the differential cross sections for Ξ^- production on ^{12}C target nucleus in the angular region of 0° – 45° by photons of energy of 2.5 GeV, calculated for two different momentum dependences of the Ξ^- hyperon effective scalar potential U_{Ξ^-} at density ρ_0 with the values $U_{\Xi^-}(0) = -24.3$ MeV and $U_{\Xi^-}(0) = -11.96$ MeV and presented in Fig. 1 as well as for zero potential at all Ξ^- momenta and without this potential, requiring that the Ξ^- hyperons go backwards in the center-of-mass system of the incident photon beam and a target nucleus at rest, as a function of Ξ^- momentum.

photon beam energy of $E_\gamma = 3.0$ GeV.

The results of calculations of the Ξ^- momentum distributions and their ratios at incident photon energy of 2.5 GeV (which is only slightly above the $KK\Xi^-$ threshold), analogous to those presented above in Figs. 5, 6 and 7, 8, are given in Figs. 9, 10 and 11, 12, respectively. It can be seen that the highest sensitivity both the Ξ^- differential cross sections and their ratios there is again in the low-momentum region of 0.1–0.8 GeV/c and this sensitivity is practically similar to that observed above at beam energy of 3.0 GeV. But at this energy the Ξ^- production cross sections are greater than those, calculated at incident energy of 2.5 GeV, by factors of about 2–4 in the low-momentum region. Therefore, they could be measured in this region at energy $E_\gamma = 3.0$ GeV to a substantially higher statistical accuracy. This is in favor of the Ξ^- momentum distribution measurements, allowing to shed light on the scalar Ξ^- -nucleus optical potential at momenta below ≈ 1.0 GeV/c, at photon energies around 3.0 GeV.

Now, we consider the effects from Ξ^- in-medium modification on the momentum dependence of the transparency ratio T_A for Ξ^- hyperons. Figures 13 and 14 show this dependence for the W/C

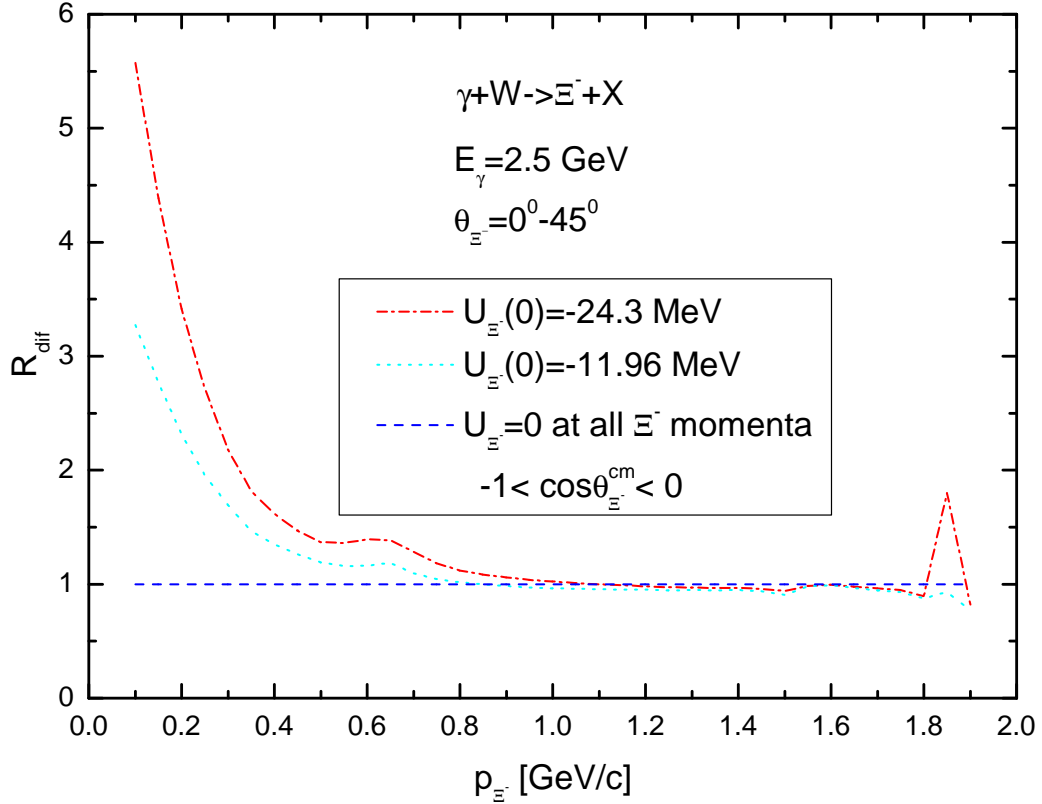


Figure 12: (Color online) The same as in Fig. 11, but for the W target nucleus.

combination for Ξ^- hyperons produced in the elementary processes (1) and (2) at laboratory polar angles $\leq 45^\circ$ by 3.0 and 2.5 GeV photons, respectively. It is calculated in line with Eq. (30) for the employed scenarios for the Ξ^- hyperon effective scalar potential U_{Ξ^-} at normal nuclear matter density ρ_0 and for the Ξ^- emission angle in the respective γp c.m.s. It is seen that for both photon energies the sensitivity of the transparency ratio T_A to the considered variations in the nuclear potential U_{Ξ^-} is low practically at all outgoing Ξ^- momenta. This means that the momentum dependence of the transparency ratio T_A for Ξ^- hyperons can hardly be used to determine this potential reliably.

Thus, we come to the conclusion that the Ξ^- differential (absolute and relative) cross section measurements in near-threshold photon-induced reactions on nuclear targets might allow one to shed light on the momentum dependence of the Ξ^- hyperon effective scalar potential in cold nuclear matter at density ρ_0 for momenta below ≈ 1.0 GeV/c. However, the transparency ratio measurements for Ξ^- hyperons in these reactions cannot serve as a reliable tool for determining this dependence.

4 Conclusions

In this paper we study the near-threshold inclusive photoproduction of Ξ^- hyperons off ^{12}C and ^{184}W target nuclei within a first-collision model relying on the nuclear spectral function and

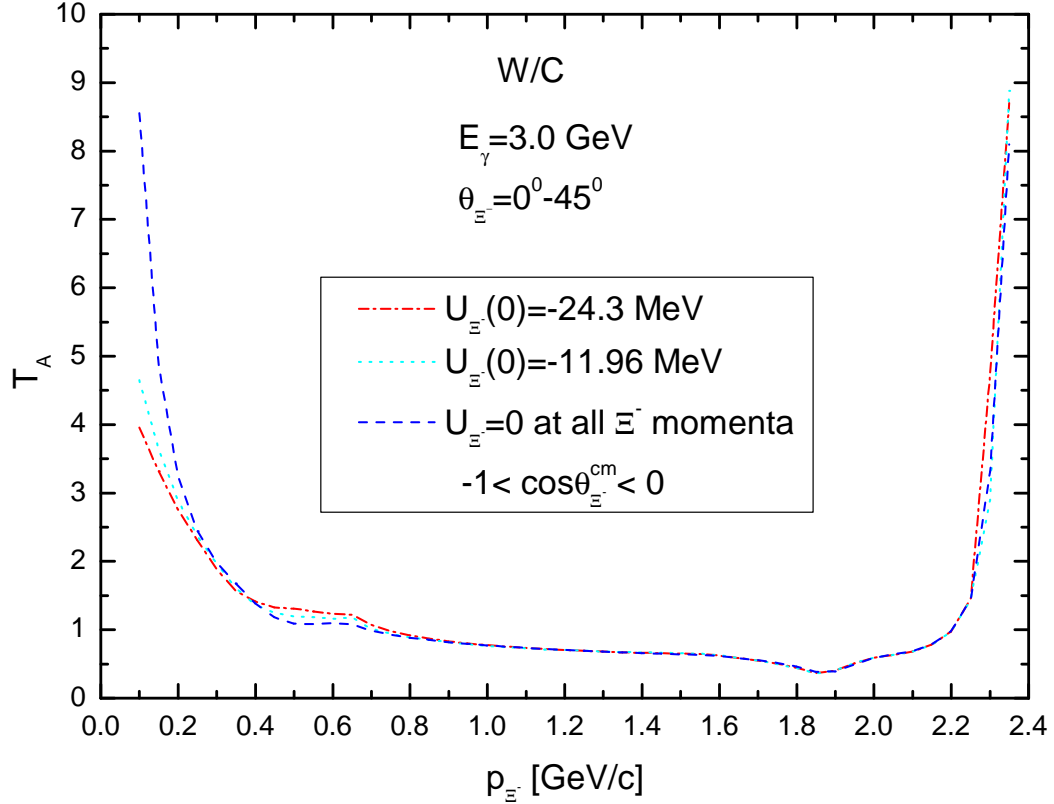


Figure 13: (Color online) Transparency ratio T_A as a function of the Ξ^- hyperon momentum for combination $^{184}\text{W}/^{12}\text{C}$ as well as for the Ξ^- laboratory polar angular range of 0° – 45° , for an incident photon energy of 3.0 GeV, calculated for two different momentum dependences of the Ξ^- hyperon effective scalar potential U_{Ξ^-} at density ρ_0 with the values $U_{\Xi^-}(0) = -24.3 \text{ MeV}$ and $U_{\Xi^-}(0) = -11.96 \text{ MeV}$ and presented in Fig. 1 as well as for zero potential at all Ξ^- momenta, requiring that the Ξ^- hyperons go backwards in the center-of-mass system of the incident photon beam and a target nucleus at rest.

including incoherent Ξ^- production in direct elementary $\gamma p \rightarrow K^+ K^+ \Xi^-$ and $\gamma n \rightarrow K^+ K^0 \Xi^-$ processes. The model takes into account the impact of the nuclear effective scalar K^+ , K^0 , Ξ^- and their Coulomb potentials on these processes as well as the absorption of final Ξ^- hyperons in nuclear matter, the binding of intranuclear nucleons and their Fermi motion. We calculate the absolute differential cross sections and their ratios for the production of Ξ^- hyperons off these nuclei at laboratory polar angles $\leq 45^\circ$ by photons with energies of 2.5 and 3.0 GeV, with and without imposing the phase space constraints on the Ξ^- emission angle in the respective γp center-of-mass system. We also calculate the momentum dependence of the transparency ratio for Ξ^- hyperons for the $^{184}\text{W}/^{12}\text{C}$ combination at these photon energies. We show that the Ξ^- momentum distributions (absolute and relative) at the adopted initial photon energies possess a definite sensitivity to the considered changes in the scalar Ξ^- nuclear mean-field potential at saturation density ρ_0 in the low-momentum range of 0.1–0.8 GeV/c. This would permit evaluating the Ξ^- potential in this momentum range experimentally. We also demonstrate that the momentum dependence of the transparency ratio for Ξ^- hyperons for both photon energies can hardly be used to determine this

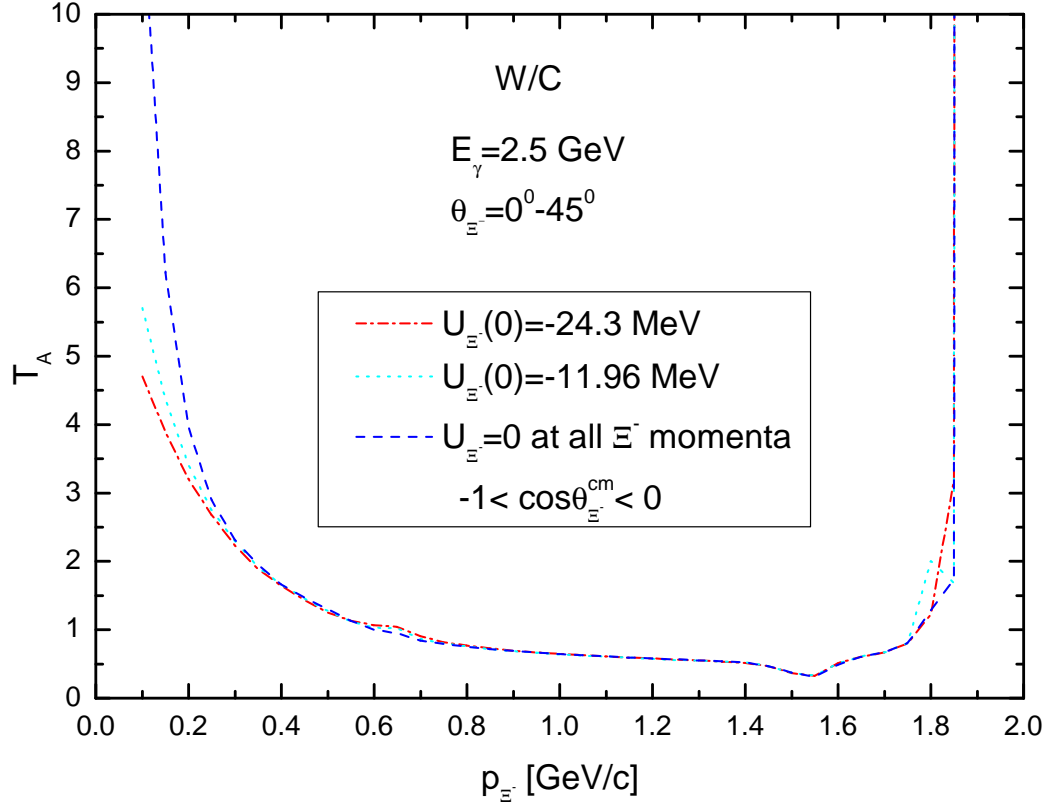


Figure 14: (Color online) The same as in Fig. 13, but for the initial photon energy of 2.5 GeV.

potential reliably. Therefore, the precise measurements of the differential cross sections (absolute and relative) for inclusive Ξ^- hyperon photoproduction on nuclei near threshold in a dedicated experiment at the CEBAF facility will provide valuable information on the Ξ^- in-medium properties, which will be supplementary to that inferred from studying of the (K^-, K^+) reactions at initial momenta of 1.6–1.8 GeV/c.

References

- [1] E. Friedman and A. Gal, Phys. Rep. **452**, 89 (2007); arXiv:0705.3965 [nucl-th].
A. Gal, E. V. Hungerford and D. J. Millener, Rev. Mod. Phys. **88**, 035004 (2016); arXiv:1605.00557 [nucl-th].
- [2] G.-C. Yong *et al.*, Phys. Lett. B **820**, 136521 (2021); arXiv:2105.10284 [nucl-th].
M. S. Abdallah *et al.* (STAR Collaboration), arXiv:2108.00924 [nucl-ex].
- [3] T. Hatsuda *et al.*, Nucl. Phys. A **967**, 856 (2017); arXiv:1704.05225 [nucl-th].
K. Sasaki *et al.* (HAL QCD Collaboration), Nucl. Phys. A **998**, 121737 (2020);

- arXiv:1912.08630 [hep-lat].
K. Sasaki *et al.* (HAL QCD Collaboration), EPJ Web Conf. **175**, 05010 (2018).
- [4] C. B. Dover and A. Gal, Annals of Phys. **146**, 309 (1983).
S. Aoki *et al.*, Phys. Lett. B **355**, 45 (1995).
- [5] K. Nakazawa *et al.*, Prog. Theor. Exp. Phys. **2015**, 033D02 (2015).
- [6] S. H. Hayakawa *et al.* (J-PARC E07 Collaboration), Phys. Rev. Lett. **126**, 062501 (2021);
arXiv:2010.14317 [nucl-ex].
- [7] M. Yoshimoto *et al.*, PTEP **2021** (7), 073D02 (2021);
arXiv:2103.08793 [nucl-ex].
- [8] J. Hu, H. Shen and Y. Zhang, arXiv:2104.13567 [nucl-th].
- [9] E. Friedman and A. Gal, Phys. Lett. B **820**, 136555 (2021);
arXiv:2104.00421 [nucl-th].
- [10] T. Fukuda *et al.*, Phys. Rev. C **58**, 1306 (1998).
- [11] P. Khaustov *et al.*, Phys. Rev. C **61**, 054603 (2000);
arXiv:nucl-ex/9912007.
- [12] T. Iijima *et al.*, Nucl. Phys. A **546**, 588 (1992).
- [13] T. Nagae *et al.* (J-PARC E05 Collaboration), PoS INPC **2016**, 038 (2017);
AIP Conf. Proc. **2130**, 020015 (2019).
- [14] T. Tamagawa, Ph.D. Thesis, University of Tokyo (unpublished) (2000).
- [15] H. Maekawa *et al.*, arXiv:0704.3929 [nucl-th].
- [16] H. Maekawa, K. Tsubakihara and A. Ohnishi, Eur. Phys. J. A **33**, 269 (2007);
arXiv:nucl-th/0701066.
- [17] T. Harada and Y. Hirabayashi, Phys. Rev. C **103**, 024605 (2021);
arXiv:2101.00855 [nucl-th].
- [18] J. Hu and H. Shen, Phys. Rev. C **96**, 054304 (2017);
arXiv:1710.08613 [nucl-th].
- [19] E. Hiyama *et al.*, Phys. Rev. C **78**, 054316 (2008);
arXiv:0811.3156 [nucl-th].
- [20] Y. Jin, X.-R. Zhou, Yi-Yu. Cheng and H.-J. Schulze, Eur. Phys. J. A **56**, 135 (2020);
arXiv:1910.05884 [nucl-th].
- [21] T. Miyatsu and K. Saito, Prog. Theor. Phys. **122**, 1035 (2009);
arXiv:0903.1893 [nucl-th].
- [22] M. Kohno and Y. Fujiwara, Phys. Rev. C **79**, 054318 (2009);
arXiv:0904.0517 [nucl-th].
- [23] M. Kohno, Phys. Rev. C **81**, 014003 (2010); arXiv:0912.4330 [nucl-th].
- [24] M. Kohno, Phys. Rev. C **100**, 024313 (2019); arXiv:1908.01934 [nucl-th].

- [25] T. Gaitanos and A. Choroziadou, Nucl. Phys. A **1008**, 122153 (2021); arXiv:2101.08470 [nucl-th].
- [26] T. Inoue (for HAL QCD Collaboration), *AIP Conf. Proc.* **2130**, no.1, 020002 (2019); arXiv:1809.08932 [hep-lat].
- [27] T. Inoue (for HAL QCD Collaboration), *PoS INPC 2016*, 277 (2016); arXiv:1612.08399 [hep-lat].
- [28] J. Haidenbauer and U.- G. Meissner, Eur. Phys. J. A **55**, 23 (2019); arXiv:1810.04883 [nucl-th].
- [29] J. Haidenbauer, U.- G. Meissner, and S. Petschauer, Nucl. Phys. A **954**, 273 (2016); arXiv:1511.05859 [nucl-th].
- [30] M. M. Nagels, Th. A. Rijken, and Y. Yamamoto, arXiv:1504.02634 [nucl-th].
- [31] H. Polinder, J. Haidenbauer, and U.-G. Meissner, Phys. Lett. B **653**, 29 (2007); arXiv:0705.3753 [nucl-th].
- [32] H. Ohnishi, F. Sakuma, and T. Takahashi, Prog. Part. Nucl. Phys. **113**, 103773 (2020); arXiv:1912.02380 [nucl-ex].
- [33] E. Ya. Paryev, Nucl. Phys. A **1013**, 122222 (2021); arXiv:2106.00353 [nucl-th].
- [34] J. W. Price *et al.* (CLAS Collaboration), Phys. Rev. C **71**, 058201 (2005); arXiv:nucl-ex/0409030.
- [35] L. Guo *et al.* (CLAS Collaboration), Phys. Rev. C **76**, 025208 (2007); arXiv:nucl-ex/0702027.
- [36] J. T. Goetz *et al.* (CLAS Collaboration), Phys. Rev. C **98**, 062201 (2018); arXiv:1809.00074 [nucl-ex].
- [37] A. Ernst and the GlueX Collaboration, AIP Conf. Proc. **2249**, 030041 (2020).
- [38] E. Ya. Paryev, M. Hartmann and Yu. T. Kiselev, J. Phys. G: Nucl. Part. Phys. **42**, 075107 (2015); arXiv:1505.01992 [nucl-th].
- [39] E. Ya. Paryev, Eur. Phys. J. A **9**, 521 (2000).
- [40] V. Metag, M. Nanova, and E. Ya. Paryev, Prog. Part. Nucl. Phys. **97**, 199 (2017); arXiv:1706.09654 [nucl-ex].
- [41] K. Tsushima *et al.*, Phys. Lett. B **429**, 239 (1998).
- [42] E. Ya. Paryev, M. Hartmann and Yu. T. Kiselev, Chinese Physics C, Vol.**41**, No.12, 124108 (2017); arXiv:1612.02767 [nucl-th].
- [43] F. Li, L.-W. Chen, C. M. Ko and S. H. Lee, Phys. Rev. C **85**, 064902 (2012); arXiv:1204.1327 [nucl-th].
- [44] G. Q. Li and C. M. Ko, Phys. Rev. C **54**, 1897 (1996); arXiv:nucl-th/9608049.
- [45] Z. Q. Feng, Phys. Rev. C **101**, 064601 (2020); arXiv:2006.02247 [nucl-th].
- [46] C.-H. Lee *et al.*, Phys. Lett. B **412**, 235 (1997); arXiv:nucl-th/9705012.

- [47] C. B. Dover and G. E. Walker, Phys. Rep. **89**, 1 (1982).
- [48] N.-Y. Ghim *et al.*, Phys. Rev. C **103**, 064306 (2021); arXiv:2102.05292 [nucl-th].
- [49] T. Tamagawa *et al.*, Nucl. Phys. A **691**, 234c (2001).
- [50] J. K. Ahn *et al.*, Phys. Lett. B **633**, 214 (2006); arXiv:nucl-ex/0502010.
- [51] J. K. Ahn and S.-il Nam, Phys. Rev. D **103**, 114022 (2021); arXiv:2101.10114 [hep-ph].
- [52] R. A. Muller, Phys. Lett. B **38**, 123 (1972).
- [53] G. R. Charlton *et al.*, Phys. Lett. B **32**, 720 (1970).
- [54] K. Nakayama, Y. Oh and H. Haberzettl, Phys. Rev. C **74**, 035205 (2006); arXiv:hep-ph/0605169.
- [55] E. Ya. Paryev, J. Phys. G: Nucl. Part. Phys. **40**, 025201 (2013); arXiv:1209.4050 [nucl-th].
- [56] E. Ya. Paryev, Chinese Physics C, Vol. **42**, No. (8), 084101 (2018); arXiv:1806.00303 [nucl-th].
- [57] S. V. Efremov and E. Ya. Paryev, Eur. Phys. J. A **1**, 99 (1998).
- [58] E. Ya. Paryev, Eur. Phys. J. A **7**, 127 (2000).
- [59] M. Nanova, S. Friedrich, V. Metag, E. Ya. Paryev *et al.*, Eur. Phys. J. A **54**, 182 (2018); arXiv:1810.01288 [nucl-ex].
- [60] J. M. Hauptman, J. A. Kadyk and G. H. Trilling, Nucl. Phys. B **125**, 29 (1977).
- [61] F. Ferro *et al.*, Nucl. Phys. A **789**, 209 (2007).